university of groningen / faculty of mathematics and natural sciences

Assessing turbulence models for large-eddy simulation using exact solutions to the Navier-Stokes equations.

Bachelor Project Mathematics

July 5, 2016

Student: Daniel Ward

Daily Supervisor: Maurits H. Silvis, MSc

First Supervisor: Prof. dr. ir. R.W.C.P. Verstappen

Second Supervisor: Dr. A.E. Sterk

Abstract

We study the behaviour of turbulent fluid flows, behaviour that is governed by the Navier-Stokes equations. Due to the extensive detail entailed in a turbulent flow, it is difficult to solve the Navier-Stokes equations numerically. A large-eddy simulation (LES), using a filtering operation, solves for the large-scale motions in a flow and smooths over small-scale motion, hence requiring a turbulence model for these small-scale motions. Using conditions derived from, and exact solutions to, the Navier-Stokes equations we investigate a number of turbulence models for LES both with and without explicit filtering. We found that the Vortex-Stretching-based eddy-viscosity model was most endorsed in the case without explicit filtering, and that the Vreman, QR, Gradient, and Vortex-Stretching-based models were equally endorsed by the case with explicit filtering, with the Smagorinsky model being the least endorsed. To reduce the bias that may arise when exact solutions are similar, we then considered classes of flows to further determine which models are the most endorsed. We considered classes based on Vreman's flow classes, and on the principal and combined invariants of flows. Once again the Vortex-Stretching-based eddy-viscosity model was usually the most endorsed. As more exact solutions to the Navier-Stokes equations are found, they can be easily added to the report to further endorse or oppose the models. We also considered Vreman's paper [16] and did not find anything to contradict his results. We did extend his results slightly by finding a solution outside of his zero-subfilter-dissipation classes with zero subfilter dissipation.

Contents

1 Introduction **4**

2 The Navier-Stokes Equations **5**
2.1 Introduction 5
2.2 Exact Solutions of the Navier-Stokes Equations 6
2.3 Characterisation of Flows 20
2.3.1 Characterising Solutions using Invariants 20
2.3.2 Vreman's Characterisation of Flows 21

3 Conditions for Large-Eddy Simulation Models **22**
3.1 Large-Eddy Simulation 22
3.2 Subfilter-Scale Models 22
3.3 Conditions for Large-Eddy Simulation without Explicit Filtering 23
3.4 Conditions for Large-Eddy Simulation with Explicit Filtering 24

4 Analysis of Large-Eddy Simulation Models **25**
4.1 Large-Eddy Simulation Without Explicit Filtering 25
4.2 Large-Eddy Simulation With Explicit Filtering 26
4.2.1 Example of a Test for a Model 27
4.2.2 Testing the Models 28
4.3 Vreman's True Subfilter Dissipation Claim 29
4.4 Classes of Flows 29
4.4.1 Vreman's Velocity Gradient Flow Classes 30
4.4.2 Vreman's Zero-True-Subfilter-Dissipation Flow Classes 31
4.4.3 Classes using the Third Principal Invariant 33
4.4.4 Two-component Flow Classes 35

5 Conclusions **37**

Appendices **39**

A Invariants of Flows **39**

B Vreman's Flow Classes **46**

C Extended Tables for Flow Classes **47**
C.1 Vreman's Velocity Gradient Flow Classes 47
C.2 Vreman's Zero-True-Subfilter-Dissipation Flow Classes 48
C.3 Classes using the Third Principal Invariant 49
C.4 Two-Component Flow Classes 50

1 Introduction

In this project we will study and test models for turbulent fluid flows. There is no all-encompassing definition of a turbulent flow, there are, however, a number of characterising properties. A turbulent flow is said to be irregular, in that it appears to be random. Turbulent flows are chaotic and hence usually described statistically due to the difficulty in a deterministic approach. Turbulent flows are diffusive, in that there is a high rate of momentum, heat, and mass transfer. They require a persistent source of input energy in order to sustain the turbulent nature of the flow, as kinetic energy is quickly converted into internal energy. A large Reynolds number is characteristic of a turbulent flow. [5]

The Navier-Stokes equations are a set of fundamental governing equations for any Newtonian fluid. An exact solution to the Navier-Stokes equations is in the form of a flow velocity and a pressure term, and hence a fluid flow can be completely described by an exact solution to the Navier-Stokes equations. It is still a non-trivial task to find such solutions, although there are a number in literature [17].

The Navier-Stokes equations have no closed form solution, resulting in difficulty when analysing complicated flows in complex geometries. This results in difficulty when solving the Navier-Stokes equations explicitly. So a mathematical model, known as Large Eddy Simulation (LES), can instead be used to model turbulent flows. LES uses what is known as a filtering operation to reduce the computational cost of a simulation by ignoring small-scale motion. What this means, however, is that information about these small-scale motions is lost. This information is often non-trivial, so subfilter-scale models (or turbulence models) are used in order to approximate the effects of small-scale motions on the large-scale fluid flow.

In this project we will use the behaviour of exact solutions to the Navier-Stokes equations to test subfilter-scale models. Applying a subfilter-scale model to a flow has two effects. One is a body force on the velocity field, called a subfilter force, and the other is a transfer of energy from large to small scales of motion, called a subfilter dissipation. This results in, respectively, an extra term being added to the Navier-Stokes equations, and to the equation of the kinetic energy of a flow.

We will then consider conditions for subfilter-scale models in two different cases. In LES without explicit filtering we will consider how a subfilter-scale model behaves for an exact solution to the Navier-Stokes equations by checking if the subfilter force and subfilter dissipation are zero for an exact solution. If so, this can be interpreted as the model being inactive, and hence this exact solution can be said to 'endorse' the model. In LES with explicit filtering we compare a model term with a term in the filtered Navier-Stokes equations (called the true turbulent stress of a flow) for exact solutions. If the two terms are both zero we will conclude that the exact solution 'strongly' endorses the model and if the two terms are both non-zero we will conclude that the exact solution 'weakly' endorses the model.

We will also consider the classification of fluid flows in order to further inspect the models and reduce the bias that may occur when solutions have similar properties. We will use properties of the invariants of a flow to characterise flows in a coordinate-independent way. Using Vreman's paper "An eddy-viscosity subgrid-scale model for turbulent shear flow: Algebraic theory and applications" [16] we will place the fluid flows into Vreman's flow classes. We will also determine whether our results say anything beyond Vreman's work.

2 The Navier-Stokes Equations

2.1 Introduction

The incompressible Navier-Stokes equations are a set of four equations that model the flow of any fluid in three-dimensional space. The standard set of Navier-Stokes equations can be written in two forms, namely by using Einstein's summation convention in what we call index notation and by using standard vector notation. In index notation they are given by

$$\frac{\partial u_i}{\partial t} + u_j \frac{\partial u_i}{\partial x_j} = -\frac{1}{\rho}\frac{\partial p}{\partial x_i} + \nu \frac{\partial^2 u_i}{\partial x_j \partial x_j}, \qquad i = 1, 2, 3;\ j = 1, 2, 3. \tag{1}$$

These equations have four variables given by the velocity of the flow $\mathbf{u} = (u_1, u_2, u_3)$, and the pressure p. The vector $\mathbf{x} = (x_1, x_2, x_3)$ represents position, t represents time, ρ corresponds to the mass density, and ν is the kinematic viscosity of the fluid.

The Navier-Stokes equations can be written in vector notation in the following way. First consider the convection term:

$$\begin{aligned} u_j \frac{\partial u_i}{\partial x_j} &\equiv \sum_{j=1}^{3} u_j \frac{\partial u_i}{\partial x_j}, \\ &= u_1 \frac{\partial u_i}{\partial x_1} + u_2 \frac{\partial u_i}{\partial x_2} + u_3 \frac{\partial u_i}{\partial x_3}, \\ &= \left(u_1 \frac{\partial}{\partial x_1} + u_2 \frac{\partial}{\partial x_2} + u_3 \frac{\partial}{\partial x_3} \right) u_i, \\ &= (\mathbf{u} \cdot \nabla) u_i. \end{aligned} \tag{2}$$

Similarly for the diffusion term:

$$\begin{aligned} \nu \frac{\partial^2 u_i}{\partial x_j \partial x_j} &\equiv \nu \sum_{j=1}^{3} \frac{\partial^2 u_i}{\partial x_j \partial x_j}, \\ &= \nu \frac{\partial^2 u_i}{\partial x_1 \partial x_1} + \frac{\partial^2 u_i}{\partial x_2 \partial x_2} + \frac{\partial^2 u_i}{\partial x_3 \partial x_3}, \\ &= \nu \left(\frac{\partial^2}{\partial x_1 \partial x_1} + \frac{\partial^2}{\partial x_2 \partial x_2} + \frac{\partial^2}{\partial x_3 \partial x_3} \right) u_i, \\ &= \nu \nabla^2 u_i. \end{aligned} \tag{3}$$

It therefore holds that, in vector notation, the Navier-Stokes equations are given by

$$\frac{\partial \mathbf{u}}{\partial t} + (\mathbf{u} \cdot \nabla)\mathbf{u} = -\frac{1}{\rho}\nabla p + \nu \nabla^2 \mathbf{u}. \tag{4}$$

It is clear that there is a problem here, there are three equations and four unknowns. In order to remedy this, the equation for conservation of mass, or the incompressibility condition, is considered. This is given by

$$\frac{\partial u_i}{\partial x_i} = 0 \tag{5}$$

in index notation, and

$$\nabla \cdot \mathbf{u} = 0 \tag{6}$$

in vector notation.

There are now four equations in four unknowns and it is possible to find solutions. Although there is no known general solution there are specific cases in which exact solutions to the Navier-Stokes equations can be found. In order to make finding solutions slightly simpler the Navier-Stokes equations can be rescaled by introducing dimensionless variables.

Let

$$u_i^* = \frac{u_i}{v}, \quad x_i^* = \frac{x_i}{\ell}, \quad t^* = \frac{t}{\ell/v}, \quad p^* = \frac{p}{\rho v^2}, \tag{7}$$

where ℓ and v are typical length and velocity scales, respectively. Then, dropping the star notation for ease of reading, the scaled incompressible Navier-Stokes equations are

$$\begin{aligned} \frac{\partial u_i}{\partial t} + u_j \frac{\partial u_i}{\partial x_j} &= -\frac{\partial p}{\partial x_i} + \frac{1}{\mathrm{Re}} \frac{\partial^2 u_i}{\partial x_j \partial x_j}, \qquad i = 1, 2, 3;\ j = 1, 2, 3; \\ \frac{\partial u_i}{\partial x_i} &= 0, \end{aligned} \tag{8}$$

where Re is the Reynolds number and is defined by the dimensionless $\mathrm{Re} = \dfrac{v\ell}{\nu}$. Similarly, in vector notation, the scaled incompressible Navier-Stokes equations are

$$\begin{aligned} \frac{\partial \mathbf{u}}{\partial t} + (\mathbf{u} \cdot \nabla)\mathbf{u} &= -\nabla p + \frac{1}{\mathrm{Re}} \nabla^2 \mathbf{u}, \\ \nabla \cdot \mathbf{u} &= 0. \end{aligned} \tag{9}$$

By multiplying the incompressible Navier-Stokes equations, Eq. (8), by u_i, and grouping terms, the differential form of the evolution of the kinetic energy of a flow can be found.

$$\frac{\partial}{\partial t}\left(\frac{1}{2} u_i u_i\right) + u_j \frac{\partial}{\partial x_j}\left(\frac{1}{2} u_i u_i\right) = -u_i \frac{\partial p}{\partial x_i} + \frac{2}{\mathrm{Re}} u_i \frac{\partial^2 u_i}{\partial x_j \partial x_j}. \tag{10}$$

The differential form of the evolution of the kinetic energy of a flow will be used later on in this report to derive conditions for the subfilter-scale models.

2.2 Exact Solutions of the Navier-Stokes Equations

By using mathematical inspection and taking results found in literature, we found a number of exact solutions to the Navier-Stokes equations. The majority are steady-state solutions, in that they are independent of time. We decided to consider exact solutions to the Navier-Stokes equations without boundary conditions in an attempt to keep the results general and applicable to a larger number of situations. All of the stated exact solutions below have been checked using a code written in Mathematica. In the solutions below the notation (x, y, z) for the Cartesian coordinate system is used analogously with (x_1, x_2, x_3), to aid in reading comprehension and in the conversion between index and vector notation.

Solution 1. Linear Velocity

If the diffusion term in the Navier-Stokes equations Eq. (1) is taken to be zero, i.e.,

$$\frac{\partial^2 u_i}{\partial x_j \partial x_j} = 0, \tag{11}$$

then each component of the velocity can be written as a linear function of x_1, x_2, and x_3. In index notation:

$$u_i = a_{ij}x_j + \beta_i. \tag{12}$$

If pressure is assumed to be a function of time t (so that the pressure terms in the Navier-Stokes equations are zero), then conditions can be found on the coefficients to find that the following is a solution.

$$\begin{aligned} u_1(x, y, z, t) &= 0, \\ u_2(x, y, z, t) &= ax + b, \\ u_3(x, y, z, t) &= cx + d, \\ p(x, y, z, t) &= f(t), \end{aligned} \tag{13}$$

where $a, b, c, d \in \mathbb{R}$, and $f : \mathbb{R} \to \mathbb{R}$. In fact, this solution is actually a specific case of Sol. 2 (Planar Flow).

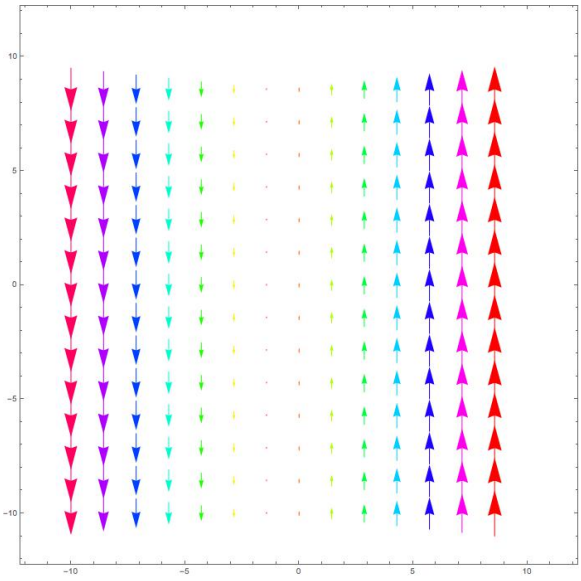

Figure 1: An illustration of the flow in the xy-plane for Sol. 1 (Linear Velocity), described in Eq. (13) with parameter values $a = b = c = d = 1$.

Solution 2. Planar Flow

Using the text by Barbato et al. [2, p.62], and modifying the solution such that it now takes three dimensions into account, another solution is found.

$$\begin{aligned} u_1(x, y, z, t) &= Az^2 + Bz + C, \\ u_2(x, y, z, t) &= Dz^2 + Ez + F, \\ u_3(x, y, z, t) &= 0, \\ p(x, y, z, t) &= \frac{2A}{\mathrm{Re}}x + \frac{2D}{\mathrm{Re}}y + f(t), \end{aligned} \tag{14}$$

where $A, B, C, D, E, F \in \mathbb{R}$ and $f : \mathbb{R} \to \mathbb{R}$. It is clear to see that if $A = D = 0$ then this is in fact the same as Eq. (13) in Sol. 1. In fact we believe (although not shown here) that this is the most general solution of the form

$$\begin{aligned} u_i(x_i, x_j, x_k, t) &= Ax_k^2 + Bx_k + C, \\ u_j(x_i, x_j, x_k, t) &= Dx_k^2 + Ex_k + F, \\ u_k(x_i, x_j, x_k, t) &= 0, \end{aligned} \tag{15}$$

for $i \neq j \neq k \neq i$.

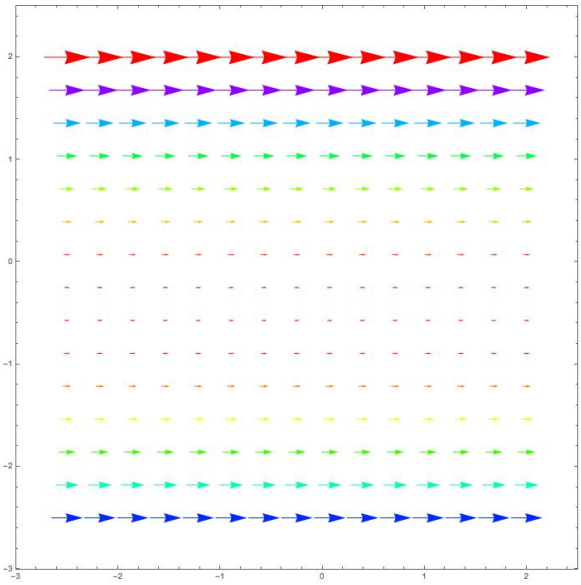

Figure 2: An illustration of the flow in the yz-plane for Sol. 2 (Planar Flow), described in Eq. (14) with parameter values $A = B = C = D = E = F = 1$.

Solution 3. Velocity as a function of time t

If each component of the velocity is taken to be a function of time t and independent of position, then the incompressibility condition is automatically satisfied. A condition can be imposed on the pressure term in order to satisfy the momentum equations. Thus a solution is as follows:

$$\begin{aligned} u_1(x, y, z, t) &= f(t), \\ u_2(x, y, z, t) &= g(t), \\ u_3(x, y, z, t) &= h(t), \\ p(x, y, z, t) &= -x\frac{\partial f(t)}{\partial t} - y\frac{\partial g(t)}{\partial t} - z\frac{\partial h(t)}{\partial t}, \end{aligned} \tag{16}$$

where $f, g, h : \mathbb{R} \to \mathbb{R}$. In fact, what is written here is the generalised Galilean transformation of the zero solution [10]. We cannot produce a plot for this flow as the functions are completely unspecified.

Solution 4. Axisymmetric Flow

Using the text by Irmay [7], a solution is defined as follows

$$\begin{aligned} u_1(x,y,z,t) &= kxz, \\ u_2(x,y,z,t) &= kyz, \\ u_3(x,y,z,t) &= -kz^2, \\ p(x,y,z,t) &= -\frac{2kz}{\mathrm{Re}} - \frac{k^2z^4}{2}, \end{aligned} \tag{17}$$

where $k \in \mathbb{R}$. This is said to represent an axisymmetric flow with hyperbolic streamlines asymptotic to the z-axis and to the boundary plane $z = 0$. These asymptotes are visible in Fig. 3.

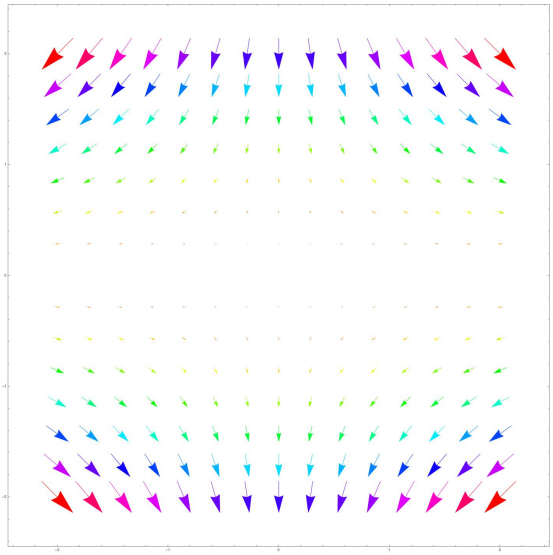

Figure 3: An illustration of the flow in the yz-plane for Sol. 4 (Axisymmetric Flow), described in Eq. (17) with parameter $k = 1$.

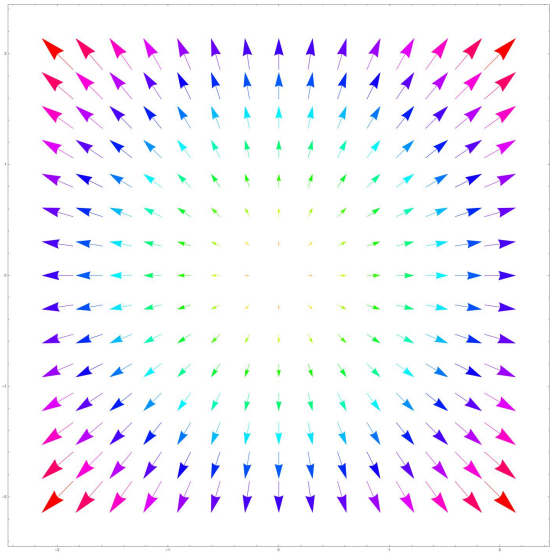

Figure 4: An illustration of the flow in the xy-plane for Sol. 4 (Axisymmetric Flow), described in Eq. (17) with parameter $k = 1$.

Solution 5. 2D Taylor Solutions

Again using the text by Barbato et al. [2, p.63–64], a solution is defined using a stream function $\psi = \psi(x, y, t)$ and by writing

$$u_1 = -\frac{\partial \psi}{\partial y}, \qquad u_2 = \frac{\partial \psi}{\partial x}, \qquad u_3 = 0. \tag{18}$$

In the text, the stream function is not given, however, it was worked out that

$$\psi = -\frac{e^{-\frac{\pi^2 t}{\mathrm{Re}}}(\cos(\pi x) + \cos(\pi y))}{\pi}. \tag{19}$$

The solution used is of the following form; note, however, that in the text the pressure term differs in that $\cos(\pi y)$ is replaced by $\sin(\pi y)$ (when testing this solution in Mathematica the solution below

was instead found).

$$
\begin{aligned}
u_1(x,y,z,t) &= -\sin(\pi y)\; e^{-\left(\pi^2 t\right)/\mathrm{Re}},\\
u_2(x,y,z,t) &= \sin(\pi x)\; e^{-\left(\pi^2 t\right)/\mathrm{Re}},\\
u_3(x,y,z,t) &= 0,\\
p(x,y,z,t) &= -\cos(\pi x)\cos(\pi y)\; e^{-\left(2\pi^2 t\right)/\mathrm{Re}}.
\end{aligned}
\tag{20}
$$

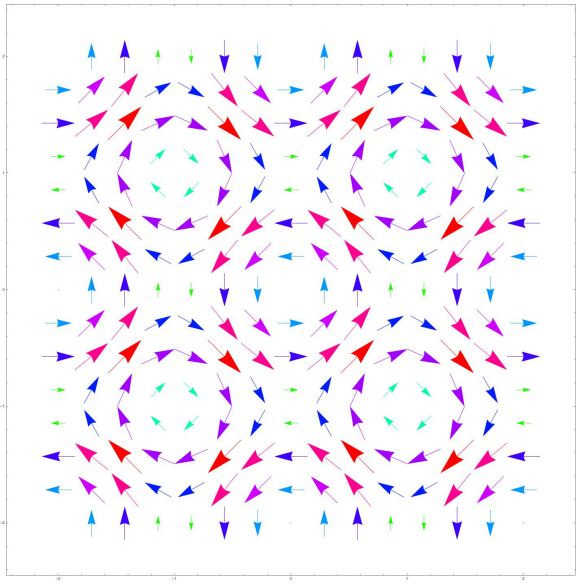

Figure 5: An illustration of the flow in the xy-plane for Sol. 5 (2D Taylor), described in Eq. (20) with $\mathrm{Re} = 1$ and time $t = 0$.

Solution 6. Generalized Beltrami Flow

Again using the text by Barbato et. al [2, p.65], and now considering solutions with non–trivial terms in all dimensions, a particular form of the generalized Beltrami flow is found, namely

$$
\begin{aligned}
u_1(x,y,z,t) &= \left(A\sin(\pi z) + C\cos(\pi y)\right)\; e^{-\left(\pi^2 t\right)/\mathrm{Re}},\\
u_2(x,y,z,t) &= \left(B\sin(\pi x) + A\cos(\pi z)\right)\; e^{-\left(\pi^2 t\right)/\mathrm{Re}},\\
u_3(x,y,z,t) &= \left(C\sin(\pi y) + B\cos(\pi x)\right)\; e^{-\left(\pi^2 t\right)/\mathrm{Re}},\\
p(x,y,z,t) &= -[(AB\cos(\pi z)\sin(\pi x) + BC\cos(\pi x)\sin(\pi y)\\
&\qquad + AC\cos(\pi y)\sin(\pi z)]\; e^{-\left(2\pi^2 t\right)/\mathrm{Re}},
\end{aligned}
\tag{21}
$$

where $A, B, C \in \mathbb{R}$.

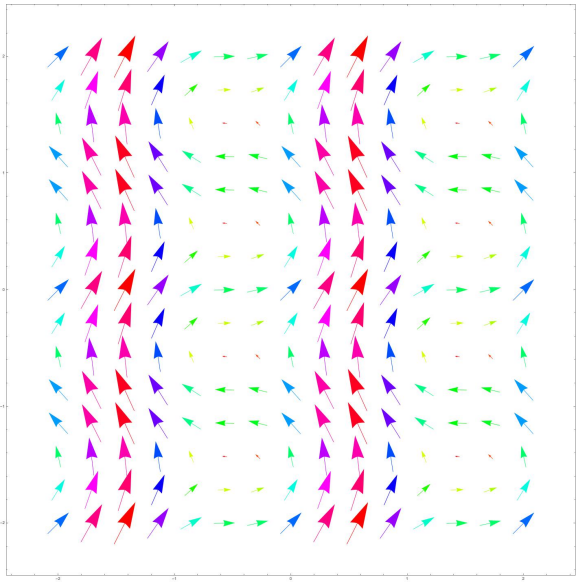

Figure 6: An illustration of the flow in the yz-plane for Sol. 6 (Generalized Beltrami Flow), described in Eq. (21) with parameters $A = B = C = 1$ and time $t = 0$.

Solution 7. Stagnation Flow

In the book by Drazin and Riley [6, p.40] an exact solution is considered which uses a stream function $\psi = \psi(y, z)$. They suggest that the following velocity field is a solution.

$$\begin{aligned} u_1(x, y, z, t) &= \frac{a}{k}x, \\ u_2(x, y, z, t) &= -\frac{a}{k}y + \frac{k}{\mathrm{Re}}\frac{\partial\psi(y, z)}{\partial z}, \\ u_3(x, y, z, t) &= -\frac{k}{\mathrm{Re}}\frac{\partial\psi(y, z)}{\partial y}. \end{aligned} \tag{22}$$

Here, we choose the stream function to be $\psi(y, z) = yz$. Then a solution is given by

$$\begin{aligned} u_1(x, y, z, t) &= \frac{a}{k}x, \\ u_2(x, y, z, t) &= \left(-\frac{a}{k} + \frac{k}{\mathrm{Re}}\right)y, \\ u_3(x, y, z, t) &= -\frac{kz}{\mathrm{Re}}, \\ p(x, y, z, t) &= -\frac{1}{2}\left(\left(\frac{ax}{k}\right)^2 - \left(\left(\frac{k}{\mathrm{Re}} - \frac{a}{k}\right)y\right)^2 - \left(\frac{kz}{\mathrm{Re}}\right)^2\right), \end{aligned} \tag{23}$$

where a is a measure of the strength of the stagnation flow and k is a constant chosen, in the text, to specify the distance between vortices. There are no vortices in this particular solution, however.

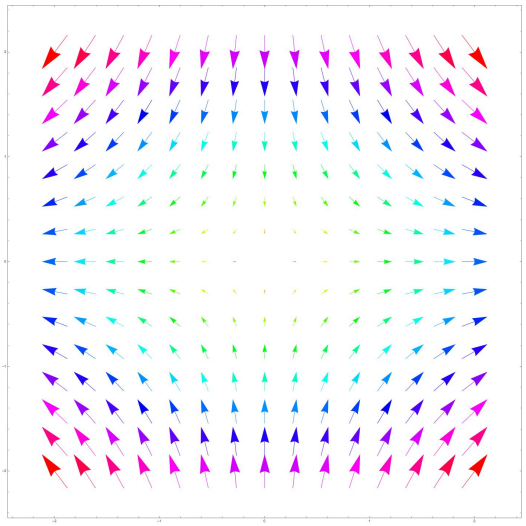

Figure 7: An illustration of the flow in the yz-plane for Sol. 7 (Stagnation Flow), described in Eq. (23) with parameter values $a = \mathrm{Re} = 1$ and $k = 2$.

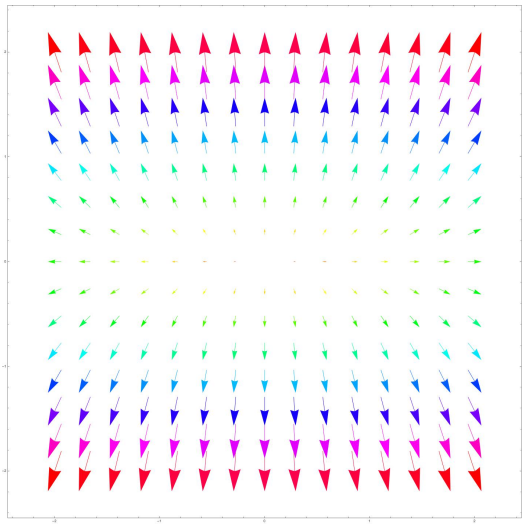

Figure 8: An illustration of the flow in the xy-plane for Sol. 7 (Stagnation Flow), described in Eq. (23) with parameter values $a = \mathrm{Re} = 1$ and $k = 2$.

Solution 8. Vortex in Stagnation Flow

As in Sol. 7 (Stagnation Flow), we now consider the same solution with a different stream function, namely $\psi(z) = \cos z$. Then, given the condition that $k = a\mathrm{Re}$, and adding a pressure term, Eq. (22) becomes

$$\begin{aligned} u_1(x, y, z, t) &= \frac{1}{\mathrm{Re}} x, \\ u_2(x, y, z, t) &= -\frac{1}{\mathrm{Re}} y - k \sin z, \\ u_3(x, y, z, t) &= 0, \\ p(x, y, z, t) &= -\frac{1}{2\mathrm{Re}^2}(x^2 + y^2), \end{aligned} \tag{24}$$

where a and k are as in Sol. 7 (Stagnation Flow).

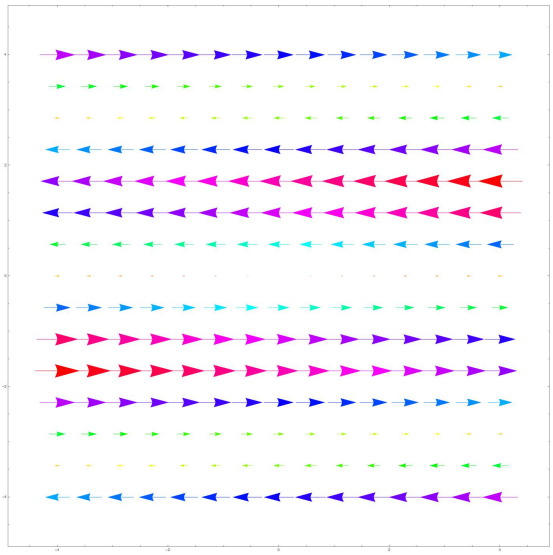

Figure 9: An illustration of the flow in the yz-plane for Sol. 8 (Vortex in Stagnation Flow), described in Eq. (24) with parameter values $k = 3$ and $\mathrm{Re} = 10$.

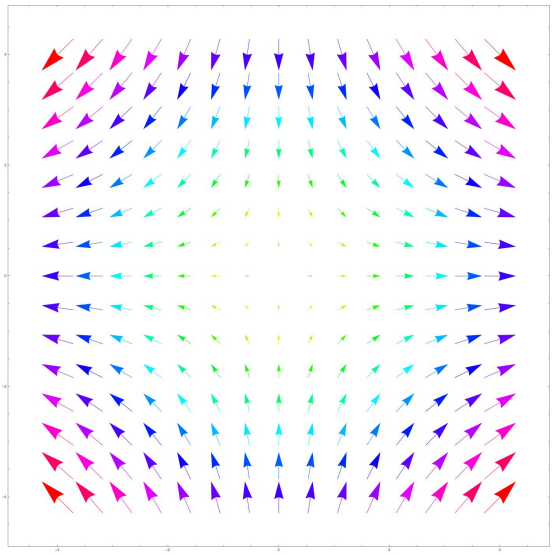

Figure 10: An illustration of the flow in the xy-plane for Sol. 8 (Vortex in Stagnation Flow), described in Eq. (24) with parameter values $k = 3$ and $\mathrm{Re} = 10$.

Solution 9. Burgers Vortex

The Burgers Vortex solution is given in cylindrical coordinates in the book by Lautrup [8, p. 385] as follows.

$$\begin{aligned} u_r(r,\varphi,z,t) &= -\frac{2r}{c^2\mathrm{Re}}, \\ u_\varphi(r,\varphi,z,t) &= \frac{\Omega c^2}{r}\left(1 - e^{-r^2/c^2}\right), \\ u_z(r,\varphi,z,t) &= \frac{4z}{c^2\mathrm{Re}}, \\ p(r,\varphi,z,t) &= -\frac{c^2\Omega^2 F\left(r^2/c^2\right)}{2} - \frac{2}{\mathrm{Re}^2}\frac{r^2+4z^2}{c^4}, \end{aligned} \tag{25}$$

where

$$F(\xi) = \int_\xi^\infty \frac{(1-e^{-x})^2}{x^2}dx. \tag{26}$$

This solution is not particularly nice to look at, however, most of the unpleasantness comes from the pressure term which (in this project) is only required in order to validate the solution. For this project all solutions are required in Cartesian coordinates, the velocity field of the Burgers Vortex has hence been converted into Cartesian coordinates.

$$\begin{aligned} u_1(x,y,z,t) &= -\frac{2x}{c^2\mathrm{Re}} - \frac{\Omega}{h(x,y)}\left(1 - \exp\left(-h(x,y)\right)\right)y, \\ u_2(x,y,z,t) &= -\frac{2y}{c^2\mathrm{Re}} + \frac{\Omega}{h(x,y)}\left(1 - \exp\left(-h(x,y)\right)\right)x, \\ u_3(x,y,z,t) &= \frac{4z}{c^2\mathrm{Re}}, \end{aligned} \tag{27}$$

where

$$h(x,y) = \frac{x^2+y^2}{c^2}, \tag{28}$$

and Ω and c are constants.

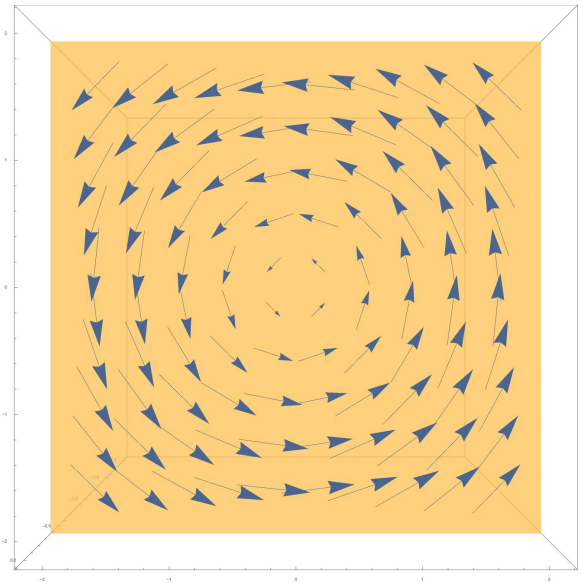

Figure 11: An illustration of the flow for Sol. 9 (Burgers Vortex), described in Eq. (27) with parameter values $c = 1.5$, $\mathrm{Re} = 20$, and $\Omega = 10$. A slice of the xy-plane at $z = 0$ is shown.

Solution 10. Another Vortex Solution

There is another vortex solution, more simply formulated than the Burgers Vortex, yet with a singularity at $r = 0$ as a result of the u_φ term. It is again given in cylindrical coordinates.

$$\begin{aligned} u_r(r,\varphi,z,t) &= -\frac{2r}{c^2\mathrm{Re}}, \\ u_\varphi(r,\varphi,z,t) &= \frac{a}{r}, \\ u_z(r,\varphi,z,t) &= \frac{4z}{c^2\mathrm{Re}}, \\ p(r,\varphi,z,t) &= -\frac{a^2}{2r^2} - \frac{2r^2+8z^2}{c^2\mathrm{Re}^2}, \end{aligned} \tag{29}$$

which can also be converted into Cartesian coordinates.

$$
\begin{aligned}
u_1(x,y,z,t) &= -\frac{2x}{c^2\mathrm{Re}} - \frac{ay}{x^2+y^2},\\
u_2(x,y,z,t) &= -\frac{2y}{c^2\mathrm{Re}} + \frac{ax}{x^2+y^2},\\
u_3(x,y,z,t) &= \frac{4z}{c^2\mathrm{Re}},
\end{aligned}
\tag{30}
$$

where a and c are constants.

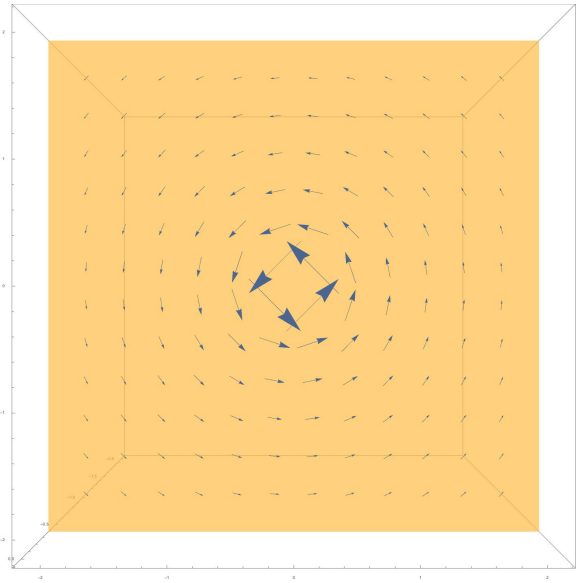

Figure 12: An illustration of the flow for Sol. 9 (Burgers Vortex), described in Eq. (27) with parameter values $c = 1.5$, $\mathrm{Re} = 20$, and $a = 10$. A slice of the xy-plane at $z = 0$ is shown.

Solution 11. Pseudo-Motion Shots of the Second Kind

In the book by Berker [3, p. 94] a solution is given in cylindrical coordinates by

$$
\begin{aligned}
u_r(r,\varphi,z,t) &= \frac{2}{\mathrm{Re}}\frac{1}{r},\\
u_\varphi(r,\varphi,z,t) &= A_1 r^3 + B_1 r + \frac{C_1}{r},\\
u_z(r,\varphi,z,t) &= A_2 r^2 \log(r) + B_2 r^2 + C_2,\\
p(r,\varphi,z,t) &= \frac{A_1^2 r^6}{6} + \frac{A_1 B_1 r^4}{2} + A_1 C_1 r^2 + \frac{B_1^2 r^2}{2} - \frac{C_1^2}{2r^2} - \frac{2}{r^2\mathrm{Re}^2} + 2B_1 C_1 \log(r)\\
&\quad + \frac{2A_2 z}{\mathrm{Re}} - \frac{4B_1\varphi}{\mathrm{Re}},
\end{aligned}
\tag{31}
$$

where $A_1, A_2, B_1, B_2, C_1, C_2$ are constants. Eq. (31), when converted into Cartesian coordinates, is

$$
\begin{aligned}
u_1(x,y,z,t) &= \frac{1}{\mathrm{Re}}\frac{2x - C_1\mathrm{Re}y}{x^2+y^2} - A_1 y\left(x^2+y^2\right) - B_1 y,\\
u_2(x,y,z,t) &= \frac{1}{\mathrm{Re}}\frac{2y + C_1\mathrm{Re}x}{x^2+y^2} + A_1 x\left(x^2+y^2\right) + B_1 x,\\
u_3(x,y,z,t) &= \frac{1}{2}A_2\left(x^2+y^2\right)\log\left(x^2+y^2\right) + B_2\left(x^2+y^2\right) + C_2.
\end{aligned}
\tag{32}
$$

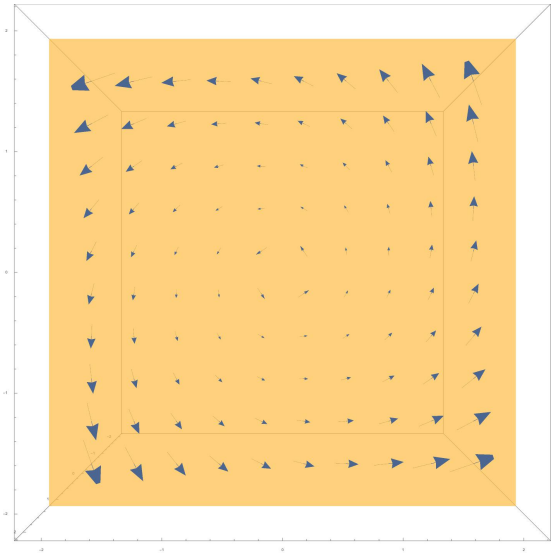

Figure 13: An illustration of the flow in the xy-plane for Sol. 11 (Pseudo-Motion Shots), described in Eqs. (31) and (32) with parameter values $A_1 = B_1 = C_1 = 1$, $A_2 = B_2 = C_2 = 2$ and $\mathrm{Re} = 10$.

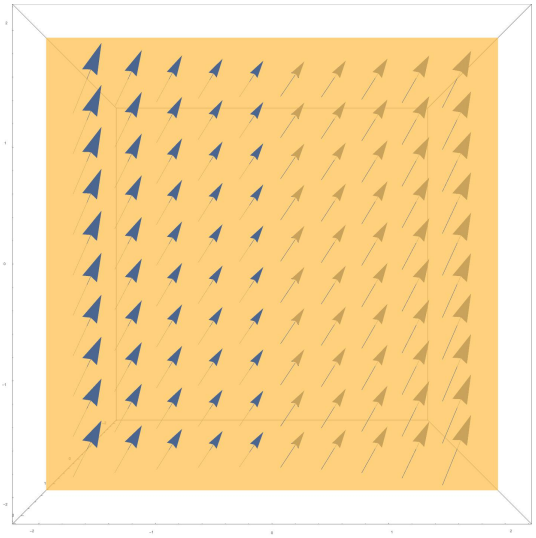

Figure 14: An illustration of the flow in the yz-plane for Sol. 11 (Pseudo-Motion Shots), described in Eqs. (31) and (32) with parameter values $A_1 = B_1 = C_1 = 1$, $A_2 = B_2 = C_2 = 2$ and $\mathrm{Re} = 10$.

Solution 12. Flows With Constant Whirl

In the book by Berker [3, p. 143] another solution is given in cylindrical coordinates by

$$
\begin{aligned}
u_r(r,\varphi,z,t) &= -\frac{1}{\mathrm{Re}}\frac{1}{r},\\
u_\varphi(r,\varphi,z,t) &= \frac{1}{r\sqrt{t}}e^{\left(-\frac{1}{2}g(t)\right)},\\
u_z(r,\varphi,z,t) &= 0,\\
p(r,\varphi,z,t) &= \frac{1}{4}\left(\frac{2\left(-\frac{e^{-g(t)}}{t} - \frac{1}{\mathrm{Re}^2}\right)}{r^2} - \frac{1}{t^2}\mathrm{Re}\int\limits_{-g(t)}^{\infty}\frac{e^{-t}}{t}dt\right).
\end{aligned}
\tag{33}
$$

where we define $g(t) = \dfrac{r^2\mathrm{Re}}{2t}$. When converted into Cartesian coordinates, we find

$$
\begin{aligned}
u_1(x,y,z,t) &= -\frac{1}{x^2+y^2}\left(\frac{y}{\sqrt{t}}\exp\left(-\frac{\mathrm{Re}\left(x^2+y^2\right)}{4t}\right)+\frac{x}{\mathrm{Re}}\right),\\
u_2(x,y,z,t) &= \frac{1}{x^2+y^2}\left(\frac{x}{\sqrt{t}}\exp\left(-\frac{\mathrm{Re}\left(x^2+y^2\right)}{4t}\right)-\frac{y}{\mathrm{Re}}\right),\\
u_3(x,y,z,t) &= 0.
\end{aligned}
\tag{34}
$$

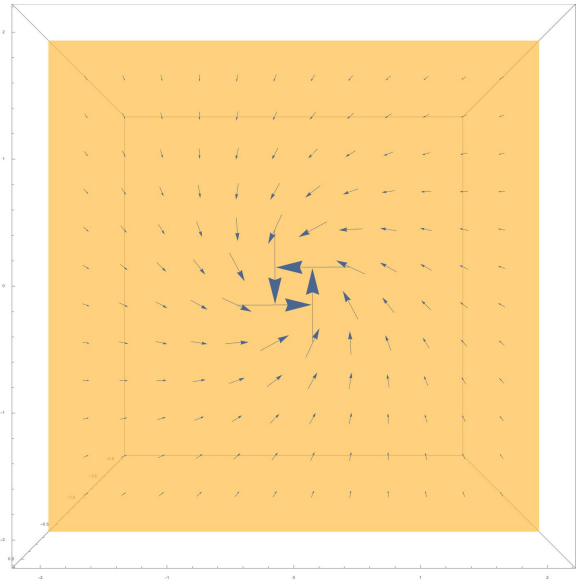

Figure 15: An illustration of the flow for Sol. 12 (Flows with Constant Whirl), described in Eqs. (33) and (34) with time $t = 1$ and $\mathrm{Re} = 1$. A slice of the xy-plane at $z = 0$ is shown, as velocity in the z-direction is zero this is the same for any value of z.

Solution 13. Rectilinear and Uniform Translation of a Sphere

In the book by Berker [3, p. 228] another solution is given in Cartesian coordinates by

$$
\begin{aligned}
u_1(x,y,z,t) &= \frac{3}{4}\frac{axz}{R^3}\left(\frac{a^2}{R^2}-1\right),\\
u_2(x,y,z,t) &= \frac{3}{4}\frac{ayz}{R^3}\left(\frac{a^2}{R^2}-1\right),\\
u_3(x,y,z,t) &= 1-\frac{3}{4}\frac{a}{R}-\frac{1}{4}\frac{a^3}{R^3}-\frac{3}{4}\frac{az^2}{R^3}\left(\frac{a^2}{R^2}-1\right),\\
p(x,y,z,t) &= \frac{3a(a-R)(a+R)}{32R^{10}\mathrm{Re}}\Big(\left(R^2\mathrm{Re}\left(x^2+y^2\right)-2R^2\mathrm{Re}z^2\right)\left(a^3+3aR^2-4R^3\right)\\
&\qquad +3a\mathrm{Re}z^4\left(R^2-a^2\right)-16R^5z\Big).
\end{aligned}
\tag{35}
$$

where a and R are constants.

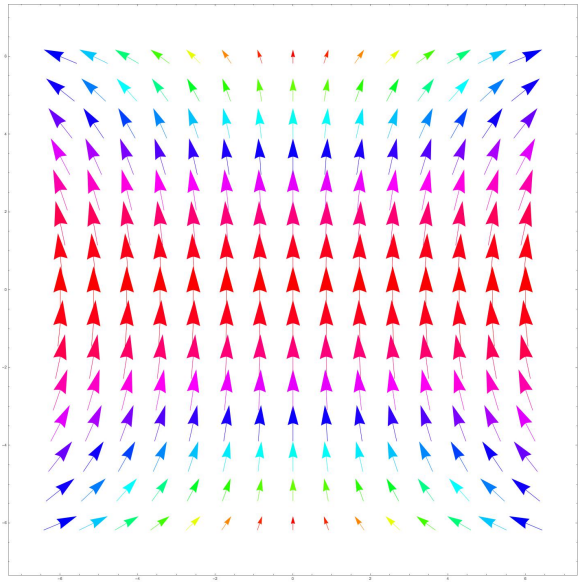

Figure 16: An illustration of the flow in the yz-plane for Sol. 13 (Sphere Translation), described in Eq. (35) with parameter values $a = -2$ and $\mathrm{Re} = 3$.

Solution 14. Radially Dependent Flow

A solution with velocity in the z-direction dependent only on the distance from the z-axis is as

follows in cylindrical coordinates.

$$\begin{aligned} u_r(r,\varphi,z,t) &= 0, \\ u_\varphi(r,\varphi,z,t) &= 0, \\ u_z(r,\varphi,z,t) &= A\left(r^2 - a^2\right), \\ p(r,\varphi,z,t) &= \frac{4Az}{\mathrm{Re}}, \end{aligned} \tag{36}$$

where A and a are constants. In Cartesian coordinates the solution is just the same with $u_1(x,y,z,t)$ and $u_2(x,y,z,t)$ both zero and the r^2 term replaced with x^2+y^2 in $u_3(x,y,z,t)$.

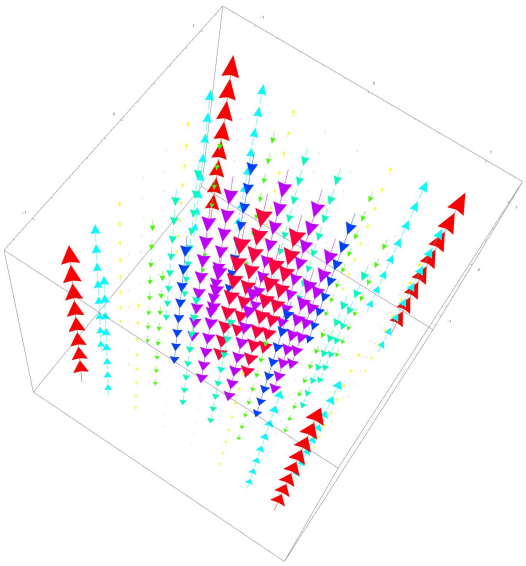

Figure 17: An illustration of the flow in 3D for Sol. 14 (Radially Dependent), described in Eq. (36) for $x,y,z \in [-1,1]$, with parameter values $a=1$, $A=4$, and $\mathrm{Re}=10$.

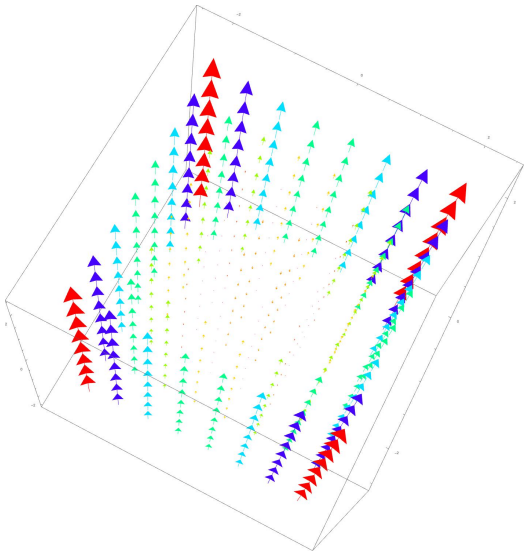

Figure 18: An illustration of the flow in 3D for Sol. 14 (Radially Dependent), described in Eq. (36) for $x,y,z \in [-2,2]$, with parameter values $a=1$, $A=4$, and $\mathrm{Re}=10$.

Solution 15. Rankine Vortex

A solution discovered by Rankine [1] is a vortex flow of the following form

$$\begin{aligned} u_r(r,\varphi,z,t) &= 0, \\ u_\varphi(r,\varphi,z,t) &= \frac{ar}{2\pi R^2}, \\ u_z(r,\varphi,z,t) &= 0, \\ p(r,\varphi,z,t) &= \frac{a^2 r^2}{8\pi^2 R^4}, \end{aligned} \tag{37}$$

where a and R are constants. In Cartesian coordinates the flow has the form

$$\begin{aligned} u_1(x,y,z,t) &= -\frac{ay}{2\pi R^2}, \\ u_2(x,y,z,t) &= \frac{ax}{2\pi R^2}, \\ u_3(x,y,z,t) &= 0, \\ p(x,y,z,t) &= \frac{a^2\left(x^2+y^2\right)}{8\pi^2 R^4}. \end{aligned} \tag{38}$$

This flow is actually a rigid body rotational flow, in that the angular rotational velocity is uniform and the velocity of the flow increases proportionally with distance from the z-axis.

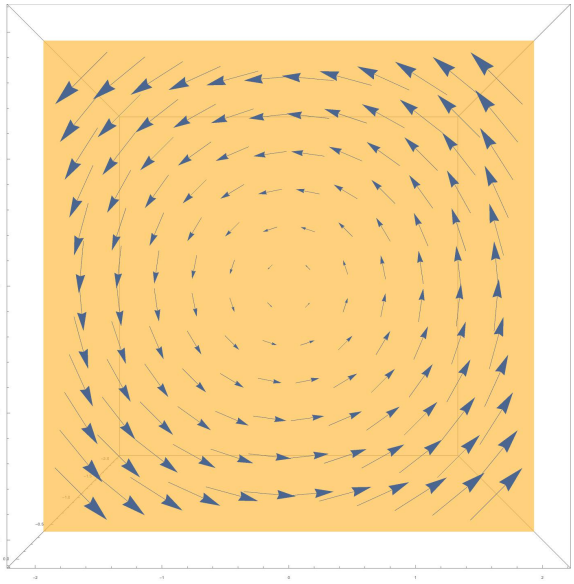

Figure 19: An illustration of the flow in the xy-plane for Sol. 15 (Rankine Vortex), described in Eq. (37) and Eq. (38) with parameter values $a = 1$ and $R = 1/\sqrt{2\pi}$.

2.3 Characterisation of Flows

It is important to be able to classify flows in a way that sorts them into distinct groups. This aids in the clear identification and general study of flows. It is also a very important way of recognising flows with similar properties. In this subsection we introduce two distinct ways in which flows can be characterised.

2.3.1 Characterising Solutions using Invariants

A principal invariant of a tensor is a coefficient of the characteristic polynomial of that tensor. Invariants, as their name suggests, are invariant under rotations of the coordinate system, in that their values do not change when the tensor is 'rotated' into a different set of coordinates. The velocity gradient of a flow, G, is defined as the Jacobian of the velocity vector, given by

$$G_{ij} = \left[\frac{\partial u_i}{\partial x_j}\right], \tag{39}$$

for $i, j = 1, 2, 3$. There are three principal invariants of the velocity gradient of a fluid flow, G, given by

$$\begin{aligned} P_G &= \mathrm{tr}(G), \\ Q_G &= \frac{1}{2}\left((\mathrm{tr}(G))^2 - \mathrm{tr}\left(G^2\right)\right), \\ R_G &= \det(G). \end{aligned} \tag{40}$$

Incompressibility of flows (Eq. (5)) ensures that $P_G = 0$, hence the first principal invariant is zero for all of the flows in Section 2.2. We now define the rate-of-strain tensor, S, by

$$S_{ij} = \frac{1}{2}\left(\frac{\partial u_i}{\partial x_j} + \frac{\partial u_j}{\partial x_i}\right), \tag{41}$$

and the rate-of-rotation tensor, Ω, by

$$\Omega_{ij} = \frac{1}{2}\left(\frac{\partial u_i}{\partial x_j} - \frac{\partial u_j}{\partial x_i}\right). \tag{42}$$

Note that the first principal invariant of S, and the first and third principal invariants of Ω are zero. Also note that the velocity gradient of a flow can simply be written $G = S + \Omega$.

Rather than considering the principal invariants, we can also consider the combined invariants:

$$I_1 = \mathrm{tr}(S^2), \quad I_2 = \mathrm{tr}(\Omega^2), \quad I_3 = \mathrm{tr}(S^3), \quad I_4 = \mathrm{tr}(S\Omega^2), \quad I_5 = \mathrm{tr}(S^2\Omega^2). \tag{43}$$

We can hence write the three principal invariants for a velocity field G in terms of the combined invariants.

$$\begin{aligned} P_G &= 0, \\ Q_G &= -\frac{1}{2}\left(I_1 + I_2\right), \\ R_G &= \frac{1}{3}\left(I_3 + 3I_4\right). \end{aligned} \tag{44}$$

In this report the flows considered are the exact solutions to the incompressible Navier-Stokes equations described in Section 2.2. The combined invariants in Eq. (43) are used to characterise these solutions into different classes in Section 4.4. Both the principal invariants and combined invariants for each exact solution in Section 2.2 are given in Appendix A.

Each of the subfilter-scale eddy-viscosity models described in Section 3.2 are written in terms of these five combined invariants.

2.3.2 Vreman's Characterisation of Flows

Vreman [16] classifies flows using the gradient of the velocity field of a flow. Each 'class' of flows has the same number of non-zero elements in the gradient matrix. For example

$$\left[\frac{\partial u_i}{\partial x_j}\right] = \begin{bmatrix} 0 & 0 & 0 \\ * & 0 & 0 \\ * & 0 & 0 \end{bmatrix}, \tag{45}$$

where a $*$ denotes a non-zero term, represents a group of flows that lie within the class denoted by $\mathcal{Q}_7$ (see Appendix B), where the subscript represents the number of non-zero terms in the velocity

gradient. Flows of the form in Eq. (45) have a velocity field of the form

$$\begin{aligned} u_1 &= c_1 \quad \text{(constant)}, \\ u_2 &= f_2(x_1), \\ u_3 &= f_3(x_1), \end{aligned} \tag{46}$$

where $f_2(x_1)$ and $f_3(x_1)$ are such that the Navier Stokes equations, Eq. (1), are satisfied. Note that as the elements on the leading diagonal are zero the incompressibility condition, Eq. (5), is automatically satisfied. Some simple flow classes are given in Appendix B and contain a number of the solutions discussed in Section 2.2. This is mentioned in greater detail in Section 4.4.1.

3 Conditions for Large-Eddy Simulation Models

3.1 Large-Eddy Simulation

Due to the nature of numerical simulation and the complexity of turbulent flows, small details are missed and information is lost when solving the Navier-Stokes equations. The computational cost of solving a turbulent flow is extremely high, so a filtering operation is applied to the Navier-Stokes equations, represented by a bar, to reduce the computational cost of the simulation. This is a linear operation and preserves constants, i.e., $\overline{\rho} = \rho$, and is also assumed to commute with differentiation,

$$\overline{\frac{\partial u_i}{\partial x_j}} = \frac{\partial \overline{u}_i}{\partial x_j}. \tag{47}$$

The filtered Navier-Stokes equations are found by filtering (putting a bar over) the entire equations (see Eq. (1)) and, after evaluating, are given by

$$\frac{\partial \overline{u}_i}{\partial t} + \overline{u}_j \frac{\partial \overline{u}_i}{\partial x_j} = -\frac{1}{\rho}\frac{\partial \overline{p}}{\partial x_i} + \nu \frac{\partial^2 \overline{u}_i}{\partial x_j \partial x_j} - \frac{\partial}{\partial x_j}\tau_{ij}, \tag{48}$$

where

$$\tau_{ij} = \overline{u_i u_j} - \overline{u}_i \overline{u}_j \tag{49}$$

is called the 'true stress' of the flow. This, however, poses a problem, as it is not clear what is meant by the term $\overline{u_i u_j}$ for a general filtering operation. The true stress τ_{ij} therefore must be replaced by a model τ_{ij}^{mod} in practical applications.

3.2 Subfilter-Scale Models

We will now define the subflter-scale models, denoted by τ_{ij}^{mod}, to be used in place of the 'difficult' true stress τ_{ij}. There are a number of models available to use in the literature [11, p.7]. These will be tested using the exact solutions to the Navier-Stokes equations and by checking conditions which are defined in Sections 3.3 and 3.4.

All the models, barring one, are of the same form. That is, each of the eddy-viscosity models are written

$$\tau_{ij}^{\text{mod}} - \frac{1}{3}\tau_{kk}^{\text{mod}}\delta_{ij} = -2\nu_e S_{ij}, \tag{50}$$

with ν_e representing the eddy viscosity of a specific model. For simplicity we usually just write $\tau_{ij}^{\text{mod}} = -2\nu_e S_{ij}$, the extra term is included here to emphasise that the models are traceless. Each

of the models we consider here can be expressed in terms of the rate of strain tensor, S, defined in Eq. (41); the rate of rotation tensor, Ω, defined in Eq. (42); and the combined invariants defined in Eq. (43). The models are then defined as follows:

$$\text{Smagorinsky [12]:} \qquad \nu_e^S = (C_S\overline{\delta})^2\sqrt{2I_1}, \tag{51}$$

$$\text{Vreman [16]:} \qquad \nu_e^V = (C_V\overline{\delta})^2\sqrt{\frac{Q_{GG^T}}{P_{GG^T}}}, \tag{52}$$

$$\text{QR [13, 14, 15]:} \qquad \nu_e^{QR} = (C_{QR}\overline{\delta})^2\frac{\max\{0,-I_3\}}{I_1}, \tag{53}$$

$$\text{Vortex-Stretching [11]:} \qquad \nu_e^{VS} = (C_{VS}\overline{\delta})^2\sqrt{2I_1}\left(\frac{I_5-\frac{1}{2}I_1I_2}{-I_1I_2}\right)^{3/2}, \tag{54}$$

with the quantities

$$P_{GG^T} = I_1 - I_2, \quad Q_{GG^T} = \frac{1}{4}(I_1+I_2)^2 + 4\left(I_5 - \frac{1}{2}I_1I_2\right). \tag{55}$$

There is a fifth and final model to be considered here. It is of a different form to the other four and not an eddy-viscosity model. It is known as the Gradient model and is defined by

$$\text{Gradient [4, 9]:} \qquad \tau_G^{\text{mod}} = C_G\overline{\delta}\left(S^2 - \Omega^2 - (S\Omega - \Omega S)\right). \tag{56}$$

The values C are model constants, specific to each model, and $\overline{\delta}$ represents the mesh size of the LES. Both of these quantities are included here to properly define the models, however, in this project they will be ignored as they are constants and have no influence on the conditions to be defined.

3.3 Conditions for Large-Eddy Simulation without Explicit Filtering

The filtering operation introduced in Eq. (48) is just a formality for LES without explicit filtering. The idea here is that filtering does not actually take place, but the term 'added' to the Navier-Stokes equations in fact 'subtracts' the difficult to simulate, small-scale turbulent motion of the flow. In order to consider this properly, the terms $\overline{u}_i$ and $\overline{p}$ in Eq. (48), are replaced by v_i and q. It is hoped that τ_{ij}^{mod} approximates τ_{ij} so that v_i and q approximate $\overline{u}_i$ and $\overline{p}$ respectively. So, LES without explicit filtering is given by

$$\frac{\partial v_i}{\partial t} + v_j\frac{\partial v_i}{\partial x_j} = -\frac{1}{\rho}\frac{\partial q}{\partial x_i} + \nu\frac{\partial^2 v_i}{\partial x_j\partial x_j} - \frac{\partial}{\partial x_j}\tau_{ij}^{\text{mod}}(v). \tag{57}$$

It is clear to see that the first four terms of this equation are exactly the same as the Navier-Stokes equations, so for the exact solutions discussed in Section 2.2, the combination of these terms will equal zero. What is then desirable is that the model term is also zero for these exact solutions, so that Eq. (57) still holds. In order to test models for exact solutions the condition

$$\frac{\partial}{\partial x_j}\tau_{ij}^{\text{mod}}(v) = 0, \tag{58}$$

is checked. If this condition were to hold it would imply that the model does not influence the velocity field of a flow, hence we call it the Velocity Field Condition. There are a number of other restrictions that can be tested. One such test comes from the differential form of the evolution of the kinetic energy of a flow, given in Eq. (10). In order to find this, Eq. (57) is multiplied by v_i and terms are grouped to find

$$\frac{\partial}{\partial t}\left(\frac{1}{2}v_iv_i\right) + v_j\frac{\partial}{\partial x_j}\left(\frac{1}{2}v_iv_i\right) = -v_i\frac{1}{\rho}\frac{\partial q}{\partial x_i} + \nu v_i\frac{\partial^2 v_i}{\partial x_j\partial x_j} - v_i\frac{\partial}{\partial x_j}\tau_{ij}^{\text{mod}}(v). \tag{59}$$

Then, similarly to Eq. (58), another condition is to check whether the model affects the kinetic energy of exact solutions, this is equivalent to checking whether

$$v_i \frac{\partial}{\partial x_j} \tau_{ij}^{\mathrm{mod}}(v) = 0. \tag{60}$$

We call this condition the Kinetic Energy Condition. The third and final condition considered here can also be found using the integral form for the equation for kinetic energy

$$\begin{aligned} \frac{d}{dt} \int_V \frac{1}{2} v_i v_i dV = \int_S \left[-v_j \left(\frac{1}{2} v_i v_i \right) - v_j \frac{q}{\rho} + 2\nu v_i S_{ij} + v_i \tau_{ij}^{\mathrm{mod}}(v) \right] n_j dS \\ + \int_V \left[-2\nu S_{ij} S_{ij} - \left(-S_{ij} \tau_{ij}^{\mathrm{mod}}(v) \right) \right] dV, \end{aligned} \tag{61}$$

where the rate-of-strain tensor S_{ij} was defined in Eq. (41). V is a volume of fluid, and dS means the integral is over the surface of that volume with unit normal n_j. Then this final condition checks whether the model affects the total kinetic energy of exact solutions to the Navier-Stokes equations, that is

$$S_{ij} \tau_{ij}^{\mathrm{mod}}(v) = 0. \tag{62}$$

We will call this condition the Dissipation Condition because $S_{ij}\tau_{ij}^{\mathrm{mod}}(v)$ is often referred to as the subgrid dissipation.

3.4 Conditions for Large-Eddy Simulation with Explicit Filtering

As in Eq. (48), the Navier-Stokes equations can be filtered by applying the filtering operation to the whole equation (putting a bar over all terms) and evaluating to find, again, that

$$\frac{\partial \overline{u}_i}{\partial t} + \overline{u}_j \frac{\partial \overline{u}_i}{\partial x_j} = -\frac{1}{\rho} \frac{\partial \overline{p}}{\partial x_i} + \nu \frac{\partial^2 \overline{u}_i}{\partial x_j \partial x_j} - \frac{\partial}{\partial x_j} \tau_{ij}. \tag{63}$$

In Eq. (57) the filtering operation was ignored and the elements $\overline{u}_i$, $\overline{p}$, and $\tau_{ij}(u)$ were replaced with v_i, q, and $\tau_{ij}^{\mathrm{mod}}(v)$ respectively. Now in LES *with* explicit filtering the filtering operation itself smooths over the small-scale turbulent motion of the simulated flow. In this case, the elements $\overline{u}_i$, $\overline{p}$, and $\tau_{ij}(u)$ will be replaced with $\overline{v}_i$, $\overline{q}$, and $\tau_{ij}^{\mathrm{mod}}(\overline{v})$ respectively. LES with explicit filtering is then given by

$$\frac{\partial \overline{v}_i}{\partial t} + \overline{v}_j \frac{\partial \overline{v}_i}{\partial x_j} = -\frac{1}{\rho} \frac{\partial \overline{q}}{\partial x_i} + \nu \frac{\partial^2 \overline{v}_i}{\partial x_j \partial x_j} - \frac{\partial}{\partial x_j} \tau_{ij}^{\mathrm{mod}}(\overline{v}). \tag{64}$$

Note that Eqs. (63) and (64), despite their similarity to Eq. (57), no longer contain the Navier-Stokes equations, as Eq. (57) did. The bar (filtering operation) over each term results in each exact solution found in Section 2.2 not necessarily satisfying the first four terms. It is hence unknown whether or not these terms will vanish for exact solutions. Terms can still be compared, similarly to Eqs. (58), (60) and (62). However, instead of comparing to zero, we can now compare to the relevant term from the filtered Navier-Stokes equations. So the terms

$$\frac{\partial}{\partial x_j} \tau_{ij} \tag{65}$$

and

$$\frac{\partial}{\partial x_j} \tau_{ij}^{\mathrm{mod}}(\overline{v}) \tag{66}$$

are to be compared. Although the latter term is relatively simple to compute, the former could lead to some difficulties due to the differentiation of the true stress $\tau_{ij} = \overline{u_i u_j} - \overline{u}_i \overline{u}_j$. So although some information could be gleaned from the inspection of these two terms, more information can be found by considering the analogue of Eq. (62). So the true subfilter dissipation

$$\overline{S}_{ij}\tau_{ij}, \tag{67}$$

(where $\overline{S}_{ij}$ is shorthand for $S_{ij}(\overline{v})$) and the modelled subfilter dissipation

$$S_{ij}(\overline{v})\tau_{ij}^{\mathrm{mod}}(\overline{v}), \tag{68}$$

are considered and have to be equal for the condition to hold. These can again be derived from the integral equation for kinetic energy of a filtered velocity field, similarly to Eq. (61).

4 Analysis of Large-Eddy Simulation Models

In this section we use a code in Mathematica, the theory described in Section 3, and the exact solutions to the Navier-Stokes equations found in Section 2.2 to check whether or not each of the exact solutions 'endorses' each model for LES both without and with explicit filtering.

4.1 Large-Eddy Simulation Without Explicit Filtering

We start by using a code in Mathematica to test the Velocity Field condition in Eq. (58) and the Kinetic Energy condition in Eq. (60). For all exact solutions to the Navier-Stokes equations in Section 2.2 the outputs for both conditions were identical so we have combined them into one table.

Velocity Field & Kinetic Energy Conditions [Do $\dfrac{\partial}{\partial x_j}\tau_{ij}^{\mathrm{mod}}(v)$ and $v_i\dfrac{\partial}{\partial x_j}\tau_{ij}^{\mathrm{mod}}(v)$ equal zero?]

Solution	1	2	3	4	5	6	7	8	9	10	11	12	13	14	15
Smagorinsky	0	*	0	*	*	*	0	*	*	*	*	*	*	*	0
Vreman	0	0	0	*	*	*	0	*	*	*	*	*	*	0	0
QR	0	0	0	*	0	*	0	*	*	*	*	0	*	0	0
Gradient	0	0	0	*	0	0	0	0	*	–	*	–	*	0	0
Vortex-Stretching	0	0	0	*	0	*	0	*	*	0	*	0	*	0	0

Table 1: For the Kinetic Energy condition a '0' result means that $v_i\frac{\partial}{\partial x_j}\tau_{ij}^{\mathrm{mod}}(v) = 0$ for respective models and exact solutions, whereas a '$*$' result means that $v_i\frac{\partial}{\partial x_j}\tau_{ij}^{\mathrm{mod}}(v) \neq 0$. For the Velocity Field condition a '0' result means that $\frac{\partial}{\partial x_j}\tau_{ij}^{\mathrm{mod}}(v) = 0$ for respective models and exact solutions, whereas a '$*$' result means that $\frac{\partial}{\partial x_j}\tau_{ij}^{\mathrm{mod}}(v) \neq 0$. The Gradient model can take both positive and negative values so when the sign of the model is known it is included in the table instead of a '*'. Both the conditions are included in one table because for all cases the outputs were identical.

We then test the Dissipation condition in Eq. (62) for all exact solutions to the Navier-Stokes equations in Section 2.2.

Dissipation Condition [Does $S_{ij}\tau_{ij}^{\text{mod}}(v) = 0$?]

Solution	1	2	3	4	5	6	7	8	9	10	11	12	13	14	15
Smagorinsky	*	*	0	*	*	*	*	*	*	*	*	*	*	*	0
Vreman	0	0	0	*	*	*	*	*	*	*	*	*	*	0	0
QR	0	0	0	*	0	*	*	*	*	*	*	0	*	0	0
Gradient	0	0	0	*	0	*	*	*	*	*	+	0	*	0	0
Vortex-Stretching	0	0	0	*	0	*	0	*	*	0	*	0	*	0	0

Table 2: A '0' result means that $S_{ij}\tau_{ij}^{\text{mod}}(v) = 0$ for respective models and exact solutions, whereas a '$*$' result means that $S_{ij}\tau_{ij}^{\text{mod}}(v) \neq 0$. The Gradient model can take both positive and negative values so when the sign of the model is known it is included in the table instead of a '*'.

We then sum all the results to find the total number of endorsements for each model described in Section 3.2.

	Smagorinsky	Vreman	QR	Gradient	Vortex-Stretching
'Velocity/Kinetic Energy' Endorsements	4	6	8	9	9
'Dissipation' Endorsements	2	5	7	7	9
Total Endorsements	6	11	15	16	18

Table 3: The results from Tables 1 and 2 are summarised to give a general overview of how many endorsements each model receives. This makes it much clearer to see the models most supported by the respective and combined conditions, with the Vortex-Stretching model being the most supported and the Smagorinsky model the least.

Testing the models in Section 3.2 using LES without explicit filtering has mixed results. It is clear that the Smagorinksy model is not well endorsed by the flows in Section 2.2, with the only endorsements coming from the simplest flows, that is Sol. 1 (Linear Velocity), Sol. 3 (Velocity as a function of time), Sol. 7 (Stagnation Flow) and Sol. 15 (Rankine Vortex). The Vortex-Stretching-based model is the most endorsed flow with eighteen out of a possible thirty endorsements. This agrees with our foreknowledge as this model was constructed to be as physically consistent as possible in the paper by Silvis & Verstappen [11].

4.2 Large-Eddy Simulation With Explicit Filtering

In this section we will compare the true subfilter dissipation $\overline{S}_{ij}\tau_{ij}$ and the modelled subfilter dissipation $S_{ij}(\overline{v})\tau_{ij}^{\text{mod}}(\overline{v})$, given in Eqs. (67) and (68) respectively, for each model τ_{ij}^{mod}, and each exact solution to the Navier-Stokes equation given in Section 2.2. We will not consider the conditions involving differentiation in Eqs. (65) and (66) due to the difficulty in calculating the derivative of the τ_{ij} term in Eq. (65).

4.2.1 Example of a Test for a Model

The true subfilter dissipation $\overline{S}_{ij}\tau_{ij}$ of a flow, given in Eq. (67), cannot be explicitly computed as the filtering operation is kept general. What can be done, however, is to partially evaluate the expressions, using the attributes of a filtering operation mentioned in Eq. (48).

The calculations of $\overline{S}_{ij}\tau_{ij}$ for Sol. 1 (Linear Velocity) are provided, to illustrate the general idea. Recall that the velocity field of Sol. 1 (Linear Velocity) is written in Eq. (13), in vector notation, as

$$u(x,y,z,t) = \begin{bmatrix} 0 \\ ax+b \\ cx+d \end{bmatrix}. \tag{69}$$

Then $\overline{S}_{ij} := S_{ij}(\overline{u})$ is computed simply by using its definition in Eq. (41). Note that as filtering preserves constants, if there is an $\overline{a}$ it is replaced with a, meaning that (in this case) there are a large number of zero terms, due to the frequency of $\overline{0}$. Hence

$$\left[S_{ij}(\overline{u})\right] = \left[\frac{1}{2}\left(\frac{\partial \overline{u}_i}{\partial x_j} + \frac{\partial \overline{u}_j}{\partial x_i}\right)\right] = \begin{bmatrix} \overline{0} & \overline{\frac{a}{2}} & \overline{\frac{c}{2}} \\ \overline{\frac{a}{2}} & \overline{0} & \overline{0} \\ \overline{\frac{c}{2}} & \overline{0} & \overline{0} \end{bmatrix} = \begin{bmatrix} 0 & \frac{a}{2} & \frac{c}{2} \\ \frac{a}{2} & 0 & 0 \\ \frac{c}{2} & 0 & 0 \end{bmatrix}. \tag{70}$$

Note that as $\overline{S}_{ij}\tau_{ij}$ is being computed, which is equal to the sum of the element-wise multiplication of the two matrices (or the trace of the matrix multiplication), that we don't need to consider the elements of $\tau_{ij}(u)$ with corresponding zero entry in $\overline{S}_{ij}$. As $\tau_{ij}(u) = \overline{u_i u_j} - \overline{u}_i\overline{u}_j$, and again, as filtering preserves constants, it is found that

$$\left[\tau_{ij}(u)\right] = \left[\overline{u_i u_j} - \overline{u}_i\overline{u}_j\right] = \begin{bmatrix} * & 0\cdot\overline{ax+b} & 0\cdot\overline{cx+d} \\ \overline{ax+b}\cdot 0 & * & * \\ \overline{cx+d}\cdot 0 & * & * \end{bmatrix} = \begin{bmatrix} * & 0 & 0 \\ 0 & * & * \\ 0 & * & * \end{bmatrix} \tag{71}$$

where a '$*$' just represents some element (not necessarily non-zero). Therefore the true subfilter dissipation

$$\overline{S}_{ij}\tau_{ij} = \operatorname{tr}\left(\begin{bmatrix} 0 & \frac{a}{2} & \frac{c}{2} \\ \frac{a}{2} & 0 & 0 \\ \frac{c}{2} & 0 & 0 \end{bmatrix} \cdot \begin{bmatrix} * & 0 & 0 \\ 0 & * & * \\ 0 & * & * \end{bmatrix}\right) = 0. \tag{72}$$

Now, the modelled subfilter dissipation $S_{ij}(\overline{u})\tau_{ij}^{\mathrm{mod}}(\overline{u})$ needs to be computed (recall that $\overline{S}_{ij} := S_{ij}(\overline{u})$). In this case, let us use the QR model, stated in Eq. (53). Once again, $S_{ij}(\overline{u})$, calculated in Eq. (70), needs to be used. So we have that

$$\tau_{ij}^{\mathrm{mod}} = -2(C_{QR}\overline{\delta})^2 \frac{\max\{0, -I_3\}}{I_1}\overline{S}_{ij}. \tag{73}$$

As

$$I_1 = \operatorname{tr}(\overline{S}^2) = \frac{1}{2}(a^2+c^2) \quad \text{and} \quad I_3 = \operatorname{tr}(\overline{S}^3) = 0 \tag{74}$$

it holds that $\tau_{ij}^{\mathrm{mod}}(\overline{u}) = 0$, so $S_{ij}(\overline{u})\tau_{ij}^{\mathrm{mod}}(\overline{u}) = 0$. This agrees with Eq. (72), and hence, Sol. 1 (Linear Velocity) endorses the QR model.

4.2.2 Testing the Models

Now, using a Mathematica code, the exact solutions in Section 2.2 are again used to evaluate the condition for the models using the process just described in Section 4.2.1. The results are described in Table 4.

Dissipation Condition 2 [Does $\overline{S}_{ij}\tau_{ij} = S_{ij}(\overline{v})\tau_{ij}^{\text{mod}}(\overline{v})$?]

Solution	1	2	3	4	5	6	7	8	9	10	11	12	13	14	15
Exact	0	0	0	*	*	*	*	*	*	*	*	*	*	0	0
Smagorinsky	*	*	0	*	*	*	*	*	*	*	*	*	*	*	0
Vreman	0	0	0	*	*	*	*	*	*	*	*	*	*	0	0
QR	0	0	0	?	0	?	?	?	?	?	?	0	?	0	0
Gradient	0	0	0	*	0	*	*	*	*	*	*	*	*	0	0
Vortex-Stretching	0	0	0	*	0	*	0	*	*	0	*	0	*	0	0

Table 4: All entries with a "0" represent a value of zero, and a "$*$" represents a value that is non-zero. The "Exact" row represents the value of the true subfilter dissipation $\overline{S}_{ij}\tau_{ij}$. Every other row with a model name represents the value of the modelled subfilter dissipation $S_{ij}(\overline{u})\tau_{ij}^{\text{mod}}(\overline{u})$, respective to that model. A "?" means that it is unclear as to the value - the sign of these values is often unknown and the 'Max' function in the definition of the QR model (in Eq. (53)) makes it difficult to evaluate.

Reading from Table 4, the Smagorinsky model is clearly endorsed by Sol. 3 (Velocity as a function of time) and Sol. 15 (Rankine Vortex) as, in both cases, both $\overline{S}_{ij}\tau_{ij} = 0 = S_{ij}(\overline{u})\tau_{ij}^{\text{mod}}(\overline{u})$. In this case we say that Sol. 3 (Velocity as a function of time) and Sol. 15 (Rankine Vortex) 'strongly' endorse the Smagorinsky model. The Smagorinsky model is not endorsed by Sol. 1 (Linear Velocity), Sol. 2 (Planar Flow), or Sol. 14 (Radially Dependent) however, because $S_{ij}(\overline{u})\tau_{ij}^{\text{mod}}(\overline{u}) \neq 0$. For Sol. 4 to 13 both $\overline{S}_{ij}\tau_{ij} \neq 0 \neq S_{ij}(\overline{u})\tau_{ij}^{\text{mod}}(\overline{u})$ and so we will say that these exact solutions 'weakly' endorse the Smagorinsky model.

	Smagorinsky	Vreman	QR	Gradient	Vortex-Stretching
'Strong' Endorsements	2	5	5	5	5
'Weak' Endorsements	10	10	?	9	6

Table 5: A 'strong' endorsement means that both $\overline{S}_{ij}\tau_{ij}$ and $S_{ij}(\overline{u})\tau_{ij}^{\text{mod}}(\overline{u})$ were found to be zero. A 'weak' endorsement means that both were found to be non-zero.

Interestingly, the 'strong' and 'weak' endorsements give different results. However, more stock should be put in the results of the 'stronger' condition as it is completely clear that zero is equal to zero. It is not necessarily clear whether or not non-zero equals non-zero as the values will depend on the parameters in each solution, hence the 'weaker' endorsement.

The 'strong' condition equally endorses the Vreman, QR, Gradient, and Vortex-Stretching-based models, whereas the 'weak' condition endorses Vreman and Smagorinsky the most, closely followed by the Gradient model, with the Vortex-Stretching-based model being the most opposed. As this

completely contradicts the 'strong' condition and the results in Section 4.1 it makes us question the validity of the weaker test. The number of endorsements for the QR model is unknown because of the definition of the model in Eq. (53) and our evaluation of the true subfilter dissipation, Eq. (67). Due to the exact solutions we have found, it is never clear whether or not the true subfilter dissipation is strictly positive or negative. This means that when the true subfilter dissipation is found to be non-zero the 'Max' function in the QR model cannot be evaluated.

4.3 Vreman's True Subfilter Dissipation Claim

Using the theory mentioned in Sections 2.3.2 and 3.4, we can place the exact solutions to the Navier-Stokes equations into different classes defined by Vreman. In doing this we can also attempt to verify one of Vreman's results [16]. In Vreman's paper he defines the class $\mathcal{Q}_n$ to be the set of flows with n zero entries in the velocity gradient of the flow (the velocity gradient is defined in Eq. (39)). Vreman then claims that the only flows with zero true subfilter dissipation are a certain selection of those in the classes $\mathcal{Q}_7$, $\mathcal{Q}_8$, or $\mathcal{Q}_9$, shown in appendix B, and is generally non-zero for any other flows.

The true subfilter dissipation of Sol. 1 (Linear Velocity) was computed in Section 4.2.1 and was found to be zero in Eq. (72). The velocity gradient of Sol. 1 is as follows

$$G_{\mathrm{LV}} = \begin{bmatrix} 0 & 0 & 0 \\ a & 0 & 0 \\ c & 0 & 0 \end{bmatrix} \tag{75}$$

and hence Sol. 1 (Linear Velocity) is in the required subset of $\mathcal{Q}_7$, which agrees with Vreman's claim. In Section 4.2.2 the true subfilter dissipation was computed (determined to be zero or non-zero) for all of the exact solutions to the Navier Stokes equations in Section 2.2. These solutions can now be 'placed' into each class. Sol. 1 (Linear Velocity), Sol. 2 (Planar Flow), Sol. 3 (Velocity as a function of time), and Sol. 14 (Radially Dependent) were all found to have zero true subfilter dissipation and are all in the appropriate subsets of either $\mathcal{Q}_7$, $\mathcal{Q}_8$ or $\mathcal{Q}_9$. This agrees with Vreman's results.

We can extend Vreman's results, however. We found that Sol. 15 (Rankine Vortex) had zero true subfilter dissipation and yet is not in the subset of $\mathcal{Q}_7$ defined in Appendix B. It is important to note that the rate of strain tensor S_{ij} in Eq. (41) for Sol. 15 (Rankine Vortex) is zero. This is the reason the true subfilter dissipation is zero and the same reason that all models are zero for this flow, as all models are based on S_{ij}.

We also found that all of the remaining exact solutions to the Navier-Stokes equations are not in Vreman's specified classes (in Appendix Section B). They also have a non-zero subfilter dissipation which agrees with Vreman's results in his paper [16].

4.4 Classes of Flows

It is important to consider that some exact solutions to the Navier-Stokes equations may have similar properties. For example, Sol. 1 (Linear Velocity) and Sol. 2 (Planar Flow) are both very similar. In fact Sol. 2 (Planar Flow) is a more general case of Sol. 1 (Linear Velocity). We therefore must group the different flows into classes in an attempt to reduce the bias that may occur when solutions are similar. This should aid us to further determine which of the models are most endorsed. We will do this in a number of different ways using the theory discussed in Section 2.3. We will group the flows with respect to Vreman's Flow Classes given in appendix B, and with respect to the Invariants given in appendix A.

4.4.1 Vreman's Velocity Gradient Flow Classes

We now put our exact solutions to the Navier-Stokes equations into one of two classes. Either $\mathcal{Q}_{0-6}$ or $\mathcal{Q}_{7-9}$, where each class is defined intuitively as follows:

$$\mathcal{Q}_{0-6} := \mathcal{Q}_0 \cup \mathcal{Q}_1 \cup \cdots \cup \mathcal{Q}_6, \tag{76}$$

$$\mathcal{Q}_{7-9} := \mathcal{Q}_7 \cup \mathcal{Q}_8 \cup \mathcal{Q}_9, \tag{77}$$

where $\mathcal{Q}_n$ is defined in Section 4.3. By looking at the gradient of each exact solution we can see that $\mathcal{Q}_{7-9}$ contains the six solutions Sol. 1 (Linear Velocity), Sol. 2 (Planar Flow), Sol. 3 (Velocity as a function of time), Sol. 5 (2D Taylor), Sol. 14 (Radially Dependent), and Sol. 15 (Rankine Vortex) and that $\mathcal{Q}_{0-6}$ contains the remaining nine. We now check the models for LES without explicit filtering by considering endorsements within each class. Tables 6 and 7 are analogues of Table 3 and illustrate the results for each flow class. The analogues of Tables 1 and 2 are Tables 22 and 23 and are in Appendix C.1.

Endorsements for models using solutions in $\mathcal{Q}_{7-9}$ for LES without explicit filtering

	Smagorinsky	Vreman	QR	Gradient	Vortex-Stretching
'Velocity/Kinetic Energy' Endorsements	3	5	6	6	6
'Dissipation' Endorsements	2	5	6	6	6
Percentage Endorsed	41.7%	83.3%	100%	100%	100%

Table 6: Each entry in the top two rows represents the number of solutions in the class $\mathcal{Q}_{7-9}$ that endorse each model. There are 6 solutions in this class so the percentages are worked out by dividing the total of each column by 12 and taking results to 1 decimal place, if necessary.

Endorsements for models using solutions in $\mathcal{Q}_{0-6}$ for LES without explicit filtering

	Smagorinsky	Vreman	QR	Gradient	Vortex-Stretching
'Velocity/Kinetic Energy' Endorsements	1	1	2	3	3
'Dissipation' Endorsements	0	0	1	0	3
Percentage Endorsed	5.6%	5.6%	16.7%	16.7%	33.3%

Table 7: Each entry in the top two rows represents the number of solutions in the class $\mathcal{Q}_{1-6}$ that endorse each model. There are 9 solutions in this class so the percentages are worked out by dividing the total of each column by 18 and taking results to 1 decimal place, if necessary.

All of the flows in the class $\mathcal{Q}_{7-9}$ endorse the QR, Gradient, and Vortex-Stretching-based subfilter-scale models (see Table 6). We can hence see that this class fully endorses these three models equally, and does not endorse the Smagorinsky model. The Vortex-Stretching eddy viscosity model has the most endorsements from any of the flows in the class $\mathcal{Q}_{0-6}$ and the Smagorinksy and Vreman models have the fewest endorsements (see Table 7). We can hence say that this class mostly endorses the Vortex-Stretching-based eddy-viscosity model, note however that the percentage endorsement is very

low.

Now let us consider LES with explicit filtering. Tables 8 and 9 are analogues of Table 5 and illustrate the results for each flow class. The analogue of Table 4 is Table 24 and is in Appendix C.1.

Endorsements for models using solutions in Q_{7-9} for LES with explicit filtering

	Smagorinsky	Vreman	QR	Gradient	Vortex-Stretching
'Strong' Endorsements	2	5	5	5	5
'Weak' Endorsements	1	1	0	0	0

Table 8: A 'strong' endorsement means that both $\overline{S}_{ij}\tau_{ij}$ and $S_{ij}(\overline{u})\tau_{ij}^{\mathrm{mod}}(\overline{u})$ were found to be zero. A 'weak' endorsement means that both were found to be non-zero.

Endorsements for models using solutions in Q_{0-6} for LES with explicit filtering

	Smagorinsky	Vreman	QR	Gradient	Vortex-Stretching
'Strong' Endorsements	0	0	0	0	0
'Weak' Endorsements	9	9	?	9	6

Table 9: A 'strong' endorsement means that both $\overline{S}_{ij}\tau_{ij}$ and $S_{ij}(\overline{u})\tau_{ij}^{\mathrm{mod}}(\overline{u})$ were found to be zero. A 'weak' endorsement means that both were found to be non-zero.

We have grouped Vreman's classes into $\mathcal{Q}_{7-9}$ and $\mathcal{Q}_{0-6}$, this is equivalent to saying that we have grouped Vreman's classes into those with two or fewer non-zero velocity gradient elements and those with three or more non-zero velocity gradient elements, respectively. Therefore the solutions in $\mathcal{Q}_{7-9}$ are exactly those with a '0' in the 'Exact' column of Table 4 and Sol. 5 (2D Taylor). Excluding Sol. 5 (2D Taylor) these are the same as those five that endorse the Vreman, QR, Gradient, and Vortex-Stretching-based models in Table 5. We can see in Table 8 that the results for the 'strong' endorsements are exactly the same as in Table 5. This is because all of the flows with zero subfilter dissipation are contained in the class $\mathcal{Q}_{7-9}$. There are hence no 'strong' endorsements in Table 9. The majority of the 'weak' endorsements come from $\mathcal{Q}_{0-6}$ as this class contains all but one of the solutions with non-zero true subfilter dissipation (given in Eq. (67)).

4.4.2 Vreman's Zero-True-Subfilter-Dissipation Flow Classes

We now separate our exact solutions into classes, again using Vreman's flow classes. This time, however, we define V_0 to be the class of flows Vreman claims will always have zero true subfilter dissipation, namely those classes mentioned in Appendix B. We define V_* to be all the remaining

classes. Then

$$V_0 = \{\text{Sol. 1 (Linear Velocity), Sol. 2 (Planar Flow),} \\ \text{Sol. 3 (Velocity as a function of time), Sol. 14 (Radially Dependent)}\}, \tag{78}$$

$$V_* = \{\text{Sol. 4 (Axisymmetric Flow), Sol. 5 (2D Taylor), Sol. 6 (Generalized Beltrami Flow),} \\ \text{Sol. 7 (Stagnation Flow), Sol. 8 (Vortex in Stagnation Flow),} \\ \text{Sol. 9 (Burgers Vortex), Sol. 10 (Another Vortex)} \\ \text{Sol. 11 (Pseudo-Motion Shots), Sol. 12 (Flows with Constant Whirl)} \\ \text{Sol. 13 (Sphere Translation), Sol. 15 (Rankine Vortex)}\}. \tag{79}$$

We now check the models for LES without explicit filtering by considering endorsements within each class. Tables 10 and 11 are analogues of Table 3 and illustrate the results for each flow class. The analogues of Tables 1 and 2 are Tables 25 and 26 and are in Appendix C.2.

Endorsements for models using solutions in V_0 for LES without explicit filtering

	Smagorinsky	Vreman	QR	Gradient	Vortex-Stretching
'Velocity/Kinetic Energy' Endorsements	2	4	4	4	4
'Dissipation' Endorsements	1	4	4	4	4
Percentage Endorsed	37.5%	100%	100%	100%	100%

Table 10: Each entry in the top two rows represents the number of solutions in the class V_0 that endorse each model. There are 4 solutions in this class so the percentages are worked out by dividing the total of each column by 8 and taking results to 1 decimal place, if necessary.

Endorsements for models using solutions in V_* for LES without explicit filtering

	Smagorinsky	Vreman	QR	Gradient	Vortex-Stretching
'Velocity/Kinetic Energy' Endorsements	2	2	4	5	5
'Dissipation' Endorsements	1	1	3	2	5
Percentage Endorsed	13.6%	13.6%	31.8%	31.8%	45.5%

Table 11: Each entry in the top two rows represents the number of solutions in the class V_* that endorse each model. There are 11 solutions in this class so the percentages are worked out by dividing the total of each column by 22 and taking results to 1 decimal place, if necessary.

All of the flows in the class V_0 endorse the Vreman, QR, Gradient, and Vortex-Stretching-based subfilter-scale models (see Table 6). This class completely endorses these four models equally and does not endorse the Smagorinsky model. The Vortex-Stretching-based eddy-viscosity model has the most endorsements from the class V_* and the Smagorinksy and Vreman models again have the fewest endorsements (see Table 7). As in Section 4.4.1 we say that this class mostly endorses the

Vortex-Stretching-based eddy-viscosity model, but once again the percentage endorsement is rather low.

Now let us consider LES with explicit filtering. Tables 12 and 13 are analogues of Table 5 and illustrate the results for each flow class. The analogue of Table 4 is Table 27 and is in Appendix C.2.

Endorsements for models using solutions in V_0 for LES with explicit filtering

	Smagorinsky	Vreman	QR	Gradient	Vortex-Stretching
'Strong' Endorsements	1	4	4	4	4
'Weak' Endorsements	0	0	0	0	0

Table 12: A 'strong' endorsement means that both $\overline{S}_{ij}\tau_{ij}$ and $S_{ij}(\overline{u})\tau_{ij}^{\mathrm{mod}}(\overline{u})$ were found to be zero. A 'weak' endorsement means that both were found to be non-zero.

Endorsements for models using solutions in V_* for LES with explicit filtering

	Smagorinsky	Vreman	QR	Gradient	Vortex-Stretching
'Strong' Endorsements	1	1	1	1	1
'Weak' Endorsements	10	10	?	9	6

Table 13: A 'strong' endorsement means that both $\overline{S}_{ij}\tau_{ij}$ and $S_{ij}(\overline{u})\tau_{ij}^{\mathrm{mod}}(\overline{u})$ were found to be zero. A 'weak' endorsement means that both were found to be non-zero.

We can see in Table 12 that the results for the 'strong' endorsements are similar to those in Table 5, excluding Sol. 15 (Rankine Vortex). The four solutions in V_0 with zero true subfilter dissipation, namely Sol. 1 (Linear Velocity), Sol. 2 (Planar Flow), Sol. 3 (Velocity as a function of time), and Sol. 14 (Radially Dependent) are hence the four that endorse the Vreman, QR, Gradient, and Vortex-Stretching-based models in Table 12. Sol. 15 (Rankine Vortex) is in the class V_* and hence there is one 'strong' endorsement in Table 13. The class V_* contains all of the flows with a non-zero true subfilter dissipation (given in Eq. (67)) and hence Table 13 contains all of the 'weak' endorsements.

4.4.3 Classes using the Third Principal Invariant

Sorting the classes using the invariants is a non-trivial task in itself. There are a number of ways in which to do this using both the principal invariants in Eq. (40) and the combined invariants in Eq. (43).

We start by looking at flows with third principal invariant R_G equal to zero. We again define two classes, R_0 and R_* where R_0 consists of all flows with $R_G = 0$ and R_* consists of all flows with $R_G \neq 0$. Then, using the information in Appendix A, we see that there are nine flows in R_0. That

is:

$$R_0 = \{\text{Sol. 1 (Linear Velocity), Sol. 2 (Planar Flow), Sol. 3 (Velocity as a function of time),}\\ \text{Sol. 5 (2D Taylor), Sol. 8 (Vortex in Stagnation Flow),}\\ \text{Sol. 11 (Pseudo-Motion Shots), Sol. 12 (Flows with Constant Whirl),}\\ \text{Sol. 14 (Radially Dependent), Sol. 15 (Rankine Vortex)}\}, \tag{80}$$

$$R_* = \{\text{Sol. 4 (Axisymmetric Flow), Sol. 6 (Generalized Beltrami Flow),}\\ \text{Sol. 7 (Stagnation Flow), Sol. 9 (Burgers Vortex), Sol. 10 (Another Vortex),}\\ \text{Sol. 13 (Sphere Translation)}\}. \tag{81}$$

We now check the models for LES without explicit filtering by considering endorsements within each class. Tables 14 and 15 are analogues of Table 3 and they illustrate the results for LES without explicit filtering for each flow class. The analogues of Tables 1 and 2 are Tables 28 and 29 and are in Appendix C.3.

Endorsements for models using solutions in R_0 for LES without explicit filtering

	Smagorinsky	Vreman	QR	Gradient	Vortex-Stretching
'Velocity/Kinetic Energy' Endorsements	3	5	7	7	7
'Dissipation' Endorsements	2	5	7	6	7
Percentage Endorsed	27.8%	55.6%	77.8%	72.2%	77.8%

Table 14: Each entry in the top two rows represents the number of solutions in the class R_0 that endorse each model. There are 9 solutions in this class so the percentages are worked out by dividing the total of each column by 18 and taking the result to one decimal place, if necessary.

Endorsements for models using solutions in R_* for LES without explicit filtering

	Smagorinsky	Vreman	QR	Gradient	Vortex-Stretching
'Velocity/Kinetic Energy' Endorsements	1	1	1	2	2
'Dissipation' Endorsements	0	0	0	0	2
Percentage Endorsed	8.3%	8.3%	8.3%	16.7%	33.3%

Table 15: Each entry in the top two rows represents the number of solutions in the class R_* that endorse each model. There are 6 solutions in this class so the percentages are worked out by dividing the total of each column by 12 and taking the result to one decimal place, if necessary.

The class R_0 endorses both the Vortex-Stretching-based model and the QR model the most and Smagorinsky the least in the case for LES without explicit filtering. In the R_* class, the Vortex-Stretching-based model is again the most endorsed followed by the Gradient model, however, the percentages are again small.

Now let us consider LES with explicit filtering. Tables 16 and 17 are analogues of Table 5 and they illustrate the results for LES with explicit filtering for each flow class. The analogue of Table 4 is Table 30 and is in Appendix C.3.

Endorsements for models using solutions in R_0 for LES with explicit filtering

	Smagorinsky	Vreman	QR	Gradient	Vortex-Stretching
'Strong' Endorsements	2	5	5	5	5
'Weak' Endorsements	4	4	?	3	2

Table 16: A 'strong' endorsement means that both $\overline{S}_{ij}\tau_{ij}$ and $S_{ij}(\overline{u})\tau_{ij}^{\text{mod}}(\overline{u})$ were found to be zero. A 'weak' endorsement means that both were found to be non-zero.

Endorsements for models using solutions in R_* for LES with explicit filtering

	Smagorinsky	Vreman	QR	Gradient	Vortex-Stretching
'Strong' Endorsements	0	0	0	0	0
'Weak' Endorsements	6	6	?	6	4

Table 17: A 'strong' endorsement means that both $\overline{S}_{ij}\tau_{ij}$ and $S_{ij}(\overline{u})\tau_{ij}^{\text{mod}}(\overline{u})$ were found to be zero. A 'weak' endorsement means that both were found to be non-zero.

As in Table 8 we can see in Table 16 that the results for the 'strong' endorsements are exactly the same as in Table 5. This is because all of the flows with zero subfilter dissipation are contained in the class R_0. As in Table 9 there are no 'strong' endorsements in Table 17. The 'weak' endorsements, however, are split more evenly between the two classes now than in Vreman's classes in Sections 4.4.1 and 4.4.2. We find that the Smagorinsky and Vreman models still seem to be the most endorsed in both classes.

4.4.4 Two-component Flow Classes

Another way in which the flows can be grouped into classes is by determining whether a flow is a two-component flow or not. We define a two-component flow to have the property that the combined principal invariants of a flow in Eq. (43) satisfy

$$I_3 = I_4 = I_5 - \frac{1}{2} I_1 I_2 = 0. \tag{82}$$

We are also interested in considering flows with zero gradient model subgrid dissipation. These flows have the property that

$$I_3 - I_4 = 0. \tag{83}$$

What we find though is that for all the solutions in Section 2.2, if a flow is a two-component flow then it also satisfies $I_3 - I_4 = 0$. It may be interesting to note that although $I_3 - I_4 \neq 0$ for many solutions, there are a number with I_3 equal to a multiple of I_4. Although not considered in this report, this may also be a class of interest. We find that the two-component flows are

$$\begin{aligned} C_2 = \{&\text{Sol. 1 (Linear Velocity), Sol. 2 (Planar Flow), Sol. 3 (Velocity as a function of time),} \\ &\text{Sol. 5 (2D Taylor), Sol. 12 (Flows with Constant Whirl),} \\ &\text{Sol. 14 (Radially Dependent), Sol. 15 (Rankine Vortex)}\}, \end{aligned} \tag{84}$$

and we call the remaining flows three-component flows. They are

$$\begin{aligned} C_3 = \{&\text{Sol. 4 (Axisymmetric Flow), Sol. 6 (Generalized Beltrami Flow),} \\ &\text{Sol. 7 (Stagnation Flow), Sol. 8 (Vortex in Stagnation Flow),} \\ &\text{Sol. 9 (Burgers Vortex), Sol. 10 (Another Vortex), Sol. 11 (Pseudo-Motion Shots),} \\ &\text{Sol. 13 (Sphere Translation)}\}. \end{aligned} \tag{85}$$

Note that Sol. 8 (Vortex in Stagnation Flow) is defined to be a planar flow, this does not mean that it is a two-component flow in this sense however because its two non-zero velocity components depend on three coordinates. We now check the models for LES without explicit filtering by considering endorsements within each class. Tables 18 and 19 are analogues of Table 3 and they illustrate the results for LES without explicit filtering for each flow class. The analogues of Tables 1 and 2 are Tables 31 and 32 and are in Appendix C.4.

Endorsements for models using solutions in C_2 for LES without explicit filtering

	Smagorinsky	Vreman	QR	Gradient	Vortex-Stretching
'Velocity/Kinetic Energy' Endorsements	3	5	7	6	7
'Dissipation' Endorsements	2	5	7	6	7
Percentage Endorsed	35.7%	71.4%	100%	85.7%	100%

Table 18: Each entry in the top two rows represents the number of solutions in the class C_2 that endorse each model. There are 7 solutions in this class so the percentages are worked out by dividing the total of each column by 14 and taking the result to one decimal place, if necessary.

Endorsements for models using solutions in C_3 for LES without explicit filtering

	Smagorinsky	Vreman	QR	Gradient	Vortex-Stretching
'Velocity/Kinetic Energy' Endorsements	1	1	1	3	2
'Dissipation' Endorsements	0	0	0	0	2
Percentage Endorsed	6.3%	6.3%	6.3%	18.8%	25.0%

Table 19: Each entry in the top two rows represents the number of solutions in the class C_3 that endorse each model. There are 8 solutions in this class so the percentages are worked out by dividing the total of each column by 16 and taking the result to one decimal place, if necessary.

The class C_2 equally endorses the QR and Vortex-Stretching-based models, and once again the Smagorinsky model is the least endorsed. As with the previous classes, the class C_3 has such low percentages that it does not seem to endorse any models. We start to see a trend appearing here, in that the flow classes that contain the more complicated flows, namely $\mathcal{Q}_{0-6}$ (Eq. (76)), V_* (Eq. (79)), R_* (Eq. (81)), and C_3 (Eq. (85)) all have very low endorsement percentages. The classes that tend to contain the simpler flows, namely $\mathcal{Q}_{7-9}$ (Eq. (77)), V_0 (Eq. (78)), R_0 (Eq. (80)), and C_2 (Eq. (84)) all seem to favour the Vortex-Stretching-based model, or the QR model.

Now let us consider LES with explicit filtering. Tables 20 and 21 are analogues of Table 5 and they illustrate the results for LES with explicit filtering for each flow class. The analogue of Table 4 is Table 33 and is in Appendix C.4.

Endorsements for models using solutions in C_2 for LES with explicit filtering

	Smagorinsky	Vreman	QR	Gradient	Vortex-Stretching
'Strong' Endorsements	2	5	5	5	5
'Weak' Endorsements	2	2	0	1	0

Table 20: A 'strong' endorsement means that both $\overline{S}_{ij}\tau_{ij}$ and $S_{ij}(\overline{u})\tau_{ij}^{\text{mod}}(\overline{u})$ were found to be zero. A 'weak' endorsement means that both were found to be non-zero.

Endorsements for models using solutions in C_3 for LES with explicit filtering

	Smagorinsky	Vreman	QR	Gradient	Vortex-Stretching
'Strong' Endorsements	0	0	0	0	0
'Weak' Endorsements	8	8	?	8	6

Table 21: A 'strong' endorsement means that both $\overline{S}_{ij}\tau_{ij}$ and $S_{ij}(\overline{u})\tau_{ij}^{\text{mod}}(\overline{u})$ were found to be zero. A 'weak' endorsement means that both were found to be non-zero.

As in Table 8 and Table 16 we can see in Table 20 that the results for the 'strong' endorsements are exactly the same as in Table 5. This is again because all of the flows with zero subfilter dissipation are contained in the class C_2. There are two flows with non-zero true subfilter dissipation (given in Eq. (67)) in C_2 and this shows in the 'weak' endorsements in Table 20. There are no 'strong' endorsements in Table 21 as all the zero subfilter dissipation flows are in C_2.

5 Conclusions

In this report we studied incompressible turbulent flows. We found a number of exact solutions to the Navier-Stokes equations, each representing a relatively simplistic fluid flow. Large-eddy simulation (LES) is used to model turbulent flows by smoothing over the complex, small-scale motion. We introduced a number of subfilter-scale models to approximate this small-scale motion and tested them using the found exact solutions to the Navier-Stokes equations. We first considered LES without explicit filtering and used the Navier-Stokes equations to derive conditions for the subfilter-scale models, namely the Velocity Field condition (Eq. (58)), the Kinetic Energy condition (Eq. (60)), and the Dissipation condition (Eq. (62)). Similarly, we considered LES with explicit filtering and again used the Navier-Stokes equations to derive more conditions for the models, in this case we decided to just take one condition, the Dissipation condition (Eqs. (67) and (68)), as the others lead to difficulty in their evaluation. By 'running' the exact solutions to the Navier-Stokes equations through each condition for the subfilter-scale models we found that the Vortex-Stretching-based eddy-viscosity model in Eq. (54) was most endorsed by the tests in LES without explicit filtering. We found that four out of the five subfilter-scale models, namely the Vreman, QR, Gradient, and Vortex-Stretching-based models were equally endorsed by the 'strong' tests in LES with explicit filtering, with the Smagorinsky model being the least endorsed. The results we found for the 'weak' condition were completely opposite to those found in both the 'strong' condition and in LES without explicit filtering. This led us to conclude that this test was not one in which we should put our trust.

We then grouped the found exact solutions into different classes in order to present more accurate results and attempt to remove bias due to similarity of exact solutions. We constructed four sets of classes, two sets with respect to Vreman's work, one with respect the the third principal invariant, and one with respect to two-component flows. We found that in the case for LES without explicit filtering, that the classes that contained the simpler flows namely $\mathcal{Q}_{7-9}$ (Eq. (77)), V_0 (Eq. (78)), R_0 (Eq. (80)), and C_2 (Eq. (84)) all seem to endorse the Vortex-Stretching-based model, or the QR model. The flow classes that tended to contain the more complicated flows, namely $\mathcal{Q}_{0-6}$ (Eq. (76)), V_* (Eq. (79)), R_* (Eq. (81)), and C_3 (Eq. (85)) all have very low endorsement percentages and hence it seems as if these classes do not endorse the flows. Despite this however, the majority still appears to lie with the Vortex-Stretching-based eddy-viscosity model. In the case for LES with explicit filtering we found for all types of classes that the flows that contribute to the 'strong' condition, namely Sol. 1 (Linear Velocity), Sol. 2 (Planar Flow), Sol. 3 (Velocity as a function of time), Sol. 14 (Radially Dependent), and Sol. 15 (Rankine Vortex) were almost always all in the simpler flow classes.

In Section 4.3 we considered Vreman's flow classes [16] and attempted to verify or extend his results. We found that fourteen out of our fifteen solutions all follow Vreman's claim that the subfilter dissipation is zero for flows in the zero-subfilter-dissipation flow classes (Appendix B). Sol. 15 (Rankine Vortex), however, extends Vreman's results in that we found a zero-subfilter-dissipation flow that is not in one of Vreman's zero-subfilter-dissipation classes.

This project could be extended by adding more exact solutions to the Navier-Stokes equations. This would result in more data for testing the models, and would also extend the flow classes found in Section 4.4. Finally, it may also be possible to design and build new eddy-viscosity models for LES by determining functions of the combined invariants in Eq. (43) for which we find that the conditions for large eddy simulation without explicit filtering in Section 3.3 and the condition for large eddy simulation with explicit filtering in Section 3.4 hold.

Appendices

A Invariants of Flows

Sol. 1 (Linear Velocity)
The principal invariants for Sol. 1 (Linear Velocity) are as follows:

$$P_G = 0, \quad Q_G = 0, \quad R_G = 0,$$

and the combined invariants are

$$I_1 = \frac{1}{2}\left(a^2 + c^2\right), \quad I_2 = -\frac{1}{2}\left(a^2 + c^2\right), \quad I_3 = 0, \quad I_4 = 0, \quad I_5 = -\frac{1}{8}\left(a^2 + c^2\right)^2.$$

Sol. 2 (Planar Flow)
The principal invariants for the Sol. 2 (Planar Flow) are the same as for Sol. 1:

$$P_G = 0, \quad Q_G = 0, \quad R_G = 0,$$

and the combined invariants are similar, in that

$$\begin{aligned}
I_1 &= \frac{1}{2}\left((2dz + e)^2 + (2gz + h)^2\right), \\
I_2 &= -\frac{1}{2}\left((2dz + e)^2 + (2gz + h)^2\right), \\
I_3 &= 0, \\
I_4 &= 0, \\
I_5 &= -\frac{1}{8}\left((2dz + e)^2 + (2gz + h)^2\right)^2.
\end{aligned}$$

Sol. 3 (Velocity as a function of time)
The principal invariants for Sol. 3 (Velocity as a function of time) are as follows:

$$P_G = 0, \quad Q_G = 0, \quad R_G = 0,$$

and the combined invariants are

$$I_1 = 0, \quad I_2 = 0, \quad I_3 = 0, \quad I_4 = 0, \quad I_5 = 0.$$

Sol. 4 (Axisymmetric Flow)
The principal invariants for Sol. 4 (Axisymmetric Flow) are as follows:

$$P_G = 0, \quad Q_G = -3a^2z^2, \quad R_G = -2a^2z^2,$$

and the combined invariants are

$$
\begin{aligned}
I_1 &= \frac{a^2}{2}\left(x^2+y^2+12z^2\right),\\
I_2 &= -\frac{a^2}{2}(x^2+y^2),\\
I_3 &= -\frac{3a^3z}{4}\left(x^2+y^2+8z^2\right),\\
I_4 &= \frac{a^3z}{4}\left(x^2+y^2\right),\\
I_5 &= -\frac{a^4}{8}\left(x^2+y^2\right)\left(x^2+y^2+10z^2\right).
\end{aligned}
$$

Sol. 5 (2D Taylor)
The principal invariants for Sol. 5 (2D Taylor) are as follows:

$$P_G = 0, \quad Q_G = \pi^2 e^{-\frac{2\pi^2 t}{R}}\cos(\pi x)\cos(\pi y), \quad R_G = 0,$$

and the combined invariants are

$$
\begin{aligned}
I_1 &= \frac{\pi^2}{2}e^{-\frac{2\pi^2 t}{R}}(\cos(\pi x)-\cos(\pi y))^2,\\
I_2 &= -\frac{\pi^2}{2}e^{-\frac{2\pi^2 t}{R}}(\cos(\pi x)+\cos(\pi y))^2,\\
I_3 &= 0,\\
I_4 &= 0,\\
I_5 &= -\frac{\pi^4}{32}e^{-\frac{4\pi^2 t}{R}}(\cos(2\pi x)-\cos(2\pi y))^2.
\end{aligned}
$$

Sol. 6 (Generalized Beltrami Flow)
The principal invariants for Sol. 6 (Generalized Beltrami Flow) are as follows:

$$
\begin{aligned}
P_G &= 0,\\
Q_G &= \pi^2 e^{-\frac{2\pi^2 t}{R}}(AB\sin(\pi x)\cos(\pi z)+AC\cos(\pi y)\sin(\pi z)+BC\cos(\pi x)\sin(\pi y)),\\
R_G &= \pi^3 ABC e^{-\frac{3\pi^2 t}{R}}(\cos(\pi x)\cos(\pi y)\cos(\pi z)-\sin(\pi x)\sin(\pi y)\sin(\pi z)),
\end{aligned}
$$

and the terms for the combined invariants are

$$I_1 = \frac{\pi^2}{2} e^{-\frac{2\pi^2 t}{R}} \left(A^2 + B^2 + C^2 - 2AB\sin(\pi x)\cos(\pi z) - 2AC\cos(\pi y)\sin(\pi z) - 2BC\cos(\pi x)\sin(\pi y)\right),$$

$$I_2 = -\frac{\pi^2}{2} e^{-\frac{2\pi^2 t}{R}} \left(A^2 + B^2 + C^2 + 2AB\sin(\pi x)\cos(\pi z) + 2AC\cos(\pi y)\sin(\pi z) + 2BC\cos(\pi x)\sin(\pi y)\right),$$

$$I_3 = \frac{3\pi^3}{4} e^{-\frac{3\pi^2 t}{R}} (A\cos(\pi z) - B\sin(\pi x))(C\cos(\pi y) - A\sin(\pi z))(B\cos(\pi x) - C\sin(\pi y)),$$

$$I_4 = \frac{\pi^3}{4} e^{-\frac{3\pi^2 t}{R}} \big(B\cos(\pi x)(C\cos(\pi y)(3A\cos(\pi z) + B\sin(\pi x)) + A\sin(\pi z)(A\cos(\pi z) - B\sin(\pi x))) +$$
$$C\sin(\pi y)(C\cos(\pi y)(A\cos(\pi z) - B\sin(\pi x)) - A\sin(\pi z)(A\cos(\pi z) + 3B\sin(\pi x)))\big),$$

$$I_5 = -\frac{\pi^4}{8} e^{-\frac{4\pi^2 t}{R}} \big(A^4 + C^2\left(B^2 - A^2\right)\cos(2\pi y) + B^2(A - C)(A + C)\cos(2\pi x)$$
$$- A(2BC(A\sin(\pi x)\cos(\pi y)\sin(2\pi z) + B\sin(2\pi x)\sin(\pi y)\cos(\pi z) + C\cos(\pi x)\sin(2\pi y)\sin(\pi z)) +$$
$$A(B - C)(B + C)\cos(2\pi z)) + B^4 + C^4\big).$$

Sol. 7 (Stagnation Flow)
The principal invariants for Sol. 7 (Stagnation Flow) are as follows:

$$P_G = 0, \quad Q_G = -\frac{a^2}{k^2} + an - k^2 n^2, \quad R_G = \frac{an\left(a - k^2 n\right)}{k},$$

and the combined invariants are

$$I_1 = \frac{2a^2}{k^2} - 2an + 2k^2 n^2, \quad I_2 = 0, \quad I_3 = \frac{3an\left(a - k^2 n\right)}{k}, \quad I_4 = 0, \quad I_5 = 0.$$

Sol. 8 (Vortex in Stagnation Flow)
The principal invariants for Sol. 8 (Vortex in Stagnation Flow) are as follows:

$$P_G = 0, \quad Q_G = -\frac{1}{\mathrm{Re}^2}, \quad R_G = 0,$$

and the combined invariants are

$$I_1 = \frac{k^2}{2}\cos^2(z) + \frac{2}{\mathrm{Re}^2},$$
$$I_2 = -\frac{k^2}{2}\cos^2(z),$$
$$I_3 = -\frac{3k^2\cos^2(z)}{4\mathrm{Re}},$$
$$I_4 = \frac{k^2\cos^2(z)}{4\mathrm{Re}},$$
$$I_5 = -\frac{k^2\cos^2(z)\left(k^2\mathrm{Re}^2\cos^2(z) + 2\right)}{8\mathrm{Re}^2}.$$

Sol. 9 (Burgers Vortex)
The principal invariants for Sol. 9 (Burgers Vortex) are as follows:

$$
\begin{aligned}
P_G &= 0, \\
Q_G &= \frac{1}{2}\Bigg(-\frac{24}{c^4\mathrm{Re}^2} - \frac{8e^{-2h(x,y)}\left(e^{h(x,y)}-1\right)^2\Omega^2x^2y^2}{h(x,y)^2} \\
&\qquad + \frac{16e^{-2h(x,y)}\left(e^{h(x,y)}-1\right)\Omega^2x^2y^2}{h(x,y)\left(x^2+y^2\right)} - \frac{8e^{-2h(x,y)}\Omega^2x^2y^2}{\left(x^2+y^2\right)^2}\Bigg) \\
R_G &= \frac{4e^{-2h(x,y)}}{c^6\mathrm{Re}^3\left(x^2+y^2\right)^2}\Bigg(e^{2h(x,y)}\left(4\left(x^2+y^2\right)^2 - c^8\mathrm{Re}^2\Omega^2\right) \\
&\qquad + 2c^6\mathrm{Re}^2\Omega^2e^{h(x,y)}\left(c^2+x^2+y^2\right) - c^6\mathrm{Re}^2\Omega^2\left(c^2+2\left(x^2+y^2\right)\right)\Bigg)
\end{aligned}
$$

where $h(x,y)$ is as defined in Eq. (28). The combined invariants are

$$
\begin{aligned}
I_1 &= \frac{2e^{-2h(x,y)}}{c^4\mathrm{Re}^2\left(x^2+y^2\right)^2}\Bigg(e^{2h(x,y)}\left(c^8\mathrm{Re}^2\Omega^2+12\left(x^2+y^2\right)^2\right) \\
&\qquad - 2c^6\mathrm{Re}^2\Omega^2e^{h(x,y)}\left(c^2+x^2+y^2\right) + c^4\mathrm{Re}^2\Omega^2\left(c^2+x^2+y^2\right)^2\Bigg), \\
I_2 &= -2\Omega^2e^{-2h(x,y)}, \\
I_3 &= \frac{1}{c^6\mathrm{Re}^3\left(x^2+y^2\right)^2}, \\
I_4 &= \frac{4\Omega^2e^{-2h(x,y)}}{c^2\mathrm{Re}}, \\
I_5 &= -\frac{2\Omega^2e^{-4h(x,y)}}{c^4\mathrm{Re}^2\left(x^2+y^2\right)^2}\Bigg(e^{2h(x,y)}\left(c^8\mathrm{Re}^2\Omega^2+4\left(x^2+y^2\right)^2\right) \\
&\qquad - 2c^6\mathrm{Re}^2\Omega^2e^{h(x,y)}\left(c^2+x^2+y^2\right) + c^4\mathrm{Re}^2\Omega^2\left(c^2+x^2+y^2\right)^2\Bigg).
\end{aligned}
$$

Sol. 10 (Another Vortex)
The principal invariants for Sol. 10 (Another Vortex) are as follows:

$$
P_G = 0, \quad Q_G = \frac{12}{c^4\mathrm{Re}^2} - \frac{d^2}{\left(x^2+y^2\right)^2}, \quad R_G = \frac{16}{c^6\mathrm{Re}^3} - \frac{4d^2}{c^2\mathrm{Re}\left(x^2+y^2\right)^2},
$$

and the combined invariants are

$$
I_1 = \frac{24}{c^4\mathrm{Re}^2} + \frac{2d^2}{\left(x^2+y^2\right)^2}, \quad I_2 = 0, \quad I_3 = \frac{48}{c^6\mathrm{Re}^3} - \frac{12d^2}{c^2\mathrm{Re}\left(x^2+y^2\right)^2}, \quad I_4 = 0, \quad I_5 = 0.
$$

Sol. 11 (Pseudo-Motion Shots)
The principal invariants for Sol. 11 (Pseudo-Motion Shots) are as follows:

$$
\begin{aligned}
P_G &= 0, \\
Q_G &= \left(A_1\left(x^2+y^2\right)+B_1\right)\left(3A_1\left(x^2+y^2\right)+B_1\right)+2A_1C_1-\frac{C_1^2\mathrm{Re}^2+4}{\mathrm{Re}^2\left(x^2+y^2\right)^2}, \\
R_G &= 0,
\end{aligned}
$$

and the combined invariants are

$$
\begin{aligned}
I_1 &= \frac{1}{2}\Bigg(\frac{\mathrm{Re}^2\left(\left(x^2+y^2\right)^3\left(4A_1^2\left(x^2+y^2\right)+(A_2+2B_2)^2\right)-8A_1C_1\left(x^2+y^2\right)^2+4C_1^2\right)+16}{\mathrm{Re}^2\left(x^2+y^2\right)^2} \\
&\qquad +A_2\left(x^2+y^2\right)\log\left(x^2+y^2\right)\left(A_2\log\left(x^2+y^2\right)+2A_2+4B_2\right)\Bigg) \\
I_2 &= -2\left(2A_1\left(x^2+y^2\right)+B_1\right)^2-\frac{1}{2}x^2\left(A_2\log\left(x^2+y^2\right)+A_2+2B_2\right)^2-\frac{1}{2}y^2\left(A_2\log\left(x^2+y^2\right)+A_2+2B_2\right)^2, \\
I_3 &= -\frac{3\left(A_2\log\left(x^2+y^2\right)+A_2+2B_2\right)^2}{2\mathrm{Re}}, \\
I_4 &= \frac{\left(A_2\log\left(x^2+y^2\right)+A_2+2B_2\right)^2}{2\mathrm{Re}}, \\
I_5 &= -\frac{1}{8\mathrm{Re}^2\left(x^2+y^2\right)}\Bigg(2A_2^2\left(\mathrm{Re}^2\left(3\left(x^2+y^2\right)^3\left(3A_1^2\left(x^2+y^2\right)+4B_2^2\right)-6A_1C_1\left(x^2+y^2\right)^2+C_1^2\right)+4\right) \\
&\quad +8A_2B_2\left(\mathrm{Re}^2\left(\left(x^2+y^2\right)^3\left(9A_1^2\left(x^2+y^2\right)+4B_2^2\right)-6A_1C_1\left(x^2+y^2\right)^2+C_1^2\right)+4\right) \\
&\quad +8\Bigg(8A_1^2\left(x^2+y^2\right)\left(\mathrm{Re}^2\left(C_1-A_1\left(x^2+y^2\right)^2\right)^2+4\right)+B_2^2\left(\mathrm{Re}^2\left(C_1-3A_1\left(x^2+y^2\right)^2\right)^2+4\right) \\
&\quad +2B_2^4\mathrm{Re}^2\left(x^2+y^2\right)^3\Bigg)+A_2^4\mathrm{Re}^2\left(x^2+y^2\right)^3+8A_2^3B_2\mathrm{Re}^2\left(x^2+y^2\right)^3\Bigg) \\
&\quad -\frac{1}{8\mathrm{Re}^2\left(x^2+y^2\right)^2}\Bigg(2B_1^2\left(\mathrm{Re}^2\left(\left(x^2+y^2\right)^3\left(8A_1^2\left(x^2+y^2\right)+(A_2+2B_2)^2\right)-16A_1C_1\left(x^2+y^2\right)^2+8C_1^2\right)+32\right) \\
&\quad +A_2\left(x^2+y^2\right)\log\left(x^2+y^2\right)\left(A_2\log\left(x^2+y^2\right)+2A_2+4B_2\right)\Big(2\big(\mathrm{Re}^2\big(\left(x^2+y^2\right)^2\big(\left(x^2+y^2\right)\left(9A_1^2\left(x^2+y^2\right)\right. \\
&\quad \left.+(A_2+2B_2)^2\right)+6A_1B_1\left(x^2+y^2\right)+B_1^2\right)-2C_1\left(x^2+y^2\right)\left(3A_1\left(x^2+y^2\right)+B_1\right)+C_1^2\big)+4\big) \\
&\quad +A_2\mathrm{Re}^2\left(x^2+y^2\right)^3\log\left(x^2+y^2\right)\left(A_2\log\left(x^2+y^2\right)+2A_2+4B_2\right)\Big) \\
&\quad +4B_1\left(x^2+y^2\right)\Big(16A_1^3\mathrm{Re}^2\left(x^2+y^2\right)^4-32A_1^2C_1\mathrm{Re}^2\left(x^2+y^2\right)^2 \\
&\quad +A_1\left(\mathrm{Re}^2\left(3(A_2+2B_2)^2\left(x^2+y^2\right)^3+16C_1^2\right)+64\right)-C_1\mathrm{Re}^2(A_2+2B_2)^2\left(x^2+y^2\right)\Big)\Bigg).
\end{aligned}
$$

Sol. 12 (Flows with Constant Whirl)
The principal invariants for Sol. 12 (Flows with Constant Whirl) are as follows:

$$P_G = 0, \quad Q_G = -\frac{\frac{2}{\mathrm{Re}^2} + \frac{1}{t^2} e^{-\frac{\mathrm{Re}\left(x^2+y^2\right)}{2t}} \left(\mathrm{Re}\left(x^2+y^2\right) + 2t\right)}{2\left(x^2+y^2\right)^2}, \quad R_G = 0,$$

and the combined invariants are

$$I_1 = \frac{e^{-\frac{\mathrm{Re}\left(x^2+y^2\right)}{2t}} \left(\mathrm{Re}^4\left(x^2+y^2\right)^2 + 8\mathrm{Re}^3 t\left(x^2+y^2\right) + 16\mathrm{Re}^2 t^2 + 16t^3 e^{\frac{\mathrm{Re}\left(x^2+y^2\right)}{2t}}\right)}{8\mathrm{Re}^2 t^3\left(x^2+y^2\right)^2},$$

$$I_2 = -\frac{\mathrm{Re}^2 e^{-\frac{\mathrm{Re}\left(x^2+y^2\right)}{2t}}}{8t^3},$$

$$I_3 = 0,$$

$$I_4 = 0,$$

$$I_5 = \frac{e^{-\frac{\mathrm{Re}\left(x^2+y^2\right)}{t}} \left(\mathrm{Re}^4\left(-\left(x^2+y^2\right)^2\right) - 8\mathrm{Re}^3 t\left(x^2+y^2\right) - 16\mathrm{Re}^2 t^2 - 16t^3 e^{\frac{\mathrm{Re}\left(x^2+y^2\right)}{2t}}\right)}{128t^6\left(x^2+y^2\right)^2}.$$

Sol. 13 (Sphere Translation)
The principal invariants for Sol. 13 (Sphere Translation) are as follows:

$$P_G = 0,$$
$$Q_G = -\frac{27a^2z^2\left(a^2-R^2\right)^2}{16R^{10}},$$
$$R_G = -\frac{27a^3z^3\left(a^2-R^2\right)^3}{32R^{15}},$$

and the combined invariants are

$$I_1 = \frac{9\left(a^3-aR^2\right)^2\left(x^2+y^2+12z^2\right)}{32R^{10}},$$
$$I_2 = -\frac{9\left(a^3-aR^2\right)^2\left(x^2+y^2\right)}{32R^{10}},$$
$$I_3 = \frac{81z\left(aR^2-a^3\right)^3\left(x^2+y^2+8z^2\right)}{256R^{15}},$$
$$I_4 = \frac{(27(a^3-aR^2)^3(x^2+y^2)z)}{(256R^15)},$$
$$I_5 = -\frac{81\left(a^3-aR^2\right)^4\left(x^2+y^2\right)\left(x^2+y^2+10z^2\right)}{2048R^{20}}.$$

Sol. 14 (Radially Dependent)
The principal invariants for Sol. 14 (Radially Dependent) are as follows:

$$P_G = 0, \quad Q_G = 0, \quad R_G = 0,$$

and the combined invariants are

$$I_1 = 2\left(x^2+y^2\right), \quad I_2 = -2\left(x^2+y^2\right), \quad I_3 = 0, \quad I_4 = 0, \quad I_5 = -2\left(x^2+y^2\right)^2.$$

Sol. 15 (Rankine Vortex)
The principal invariants for Sol. 15 (Rankine Vortex) are as follows:

$$P_G = 0, \quad Q_G = 0, \quad R_G = 0,$$

and the combined invariants are

$$I_1 = 0, \quad I_2 = -\frac{a^2}{2\pi^2 R^4}, \quad I_3 = 0, \quad I_4 = 0, \quad I_5 = 0.$$

B Vreman's Flow Classes

In his paper [16], Vreman claims that there are 13 classes of flows for which the true subfilter dissipation equals zero. The classes are all subsets of $\mathcal{Q}_7, \mathcal{Q}_8$ and $\mathcal{Q}_9$ where $\mathcal{Q}_n$, with $n \in [0, 9]$, is defined to be the class of flows with zero entries in the velocity gradient of the flow (defined in Eq. (39)). Below are the flow classes claimed to have zero true subfilter dissipation.

$$\left\{ \begin{bmatrix} 0 & 0 & 0 \\ 0 & 0 & 0 \\ 0 & 0 & 0 \end{bmatrix} \right\} \subseteq \mathcal{Q}_9.$$

$$\left\{ \begin{bmatrix} 0 & 0 & 0 \\ * & 0 & 0 \\ 0 & 0 & 0 \end{bmatrix}, \begin{bmatrix} 0 & * & 0 \\ 0 & 0 & 0 \\ 0 & 0 & 0 \end{bmatrix}, \begin{bmatrix} 0 & 0 & 0 \\ 0 & 0 & 0 \\ * & 0 & 0 \end{bmatrix}, \right.$$
$$\left. \begin{bmatrix} 0 & 0 & * \\ 0 & 0 & 0 \\ 0 & 0 & 0 \end{bmatrix}, \begin{bmatrix} 0 & 0 & 0 \\ 0 & 0 & 0 \\ 0 & * & 0 \end{bmatrix}, \begin{bmatrix} 0 & 0 & 0 \\ 0 & 0 & * \\ 0 & 0 & 0 \end{bmatrix} \right\} \subseteq \mathcal{Q}_8.$$

$$\left\{ \begin{bmatrix} 0 & 0 & 0 \\ * & 0 & 0 \\ * & 0 & 0 \end{bmatrix}, \begin{bmatrix} 0 & * & 0 \\ 0 & 0 & 0 \\ 0 & * & 0 \end{bmatrix}, \begin{bmatrix} 0 & 0 & * \\ 0 & 0 & * \\ 0 & 0 & 0 \end{bmatrix}, \right.$$
$$\left. \begin{bmatrix} 0 & * & * \\ 0 & 0 & 0 \\ 0 & 0 & 0 \end{bmatrix}, \begin{bmatrix} 0 & 0 & 0 \\ * & 0 & * \\ 0 & 0 & 0 \end{bmatrix}, \begin{bmatrix} 0 & 0 & 0 \\ 0 & 0 & 0 \\ * & * & 0 \end{bmatrix} \right\} \subseteq \mathcal{Q}_7.$$

C Extended Tables for Flow Classes

C.1 Vreman's Velocity Gradient Flow Classes

Velocity Field & Kinetic Energy Conditions [Do $\frac{\partial}{\partial x_j}\tau_{ij}^{\mathrm{mod}}(v)$ and $v_i\frac{\partial}{\partial x_j}\tau_{ij}^{\mathrm{mod}}(v)$ equal zero?]

	$\mathcal{Q}_{7-9}$						$\mathcal{Q}_{0-6}$								
Solution	1	2	3	5	14	15	4	6	7	8	9	10	11	12	13
Smagorinsky	0	*	0	*	*	0	*	*	0	*	*	*	*	*	*
Vreman	0	0	0	*	0	0	*	*	0	*	*	*	*	*	*
QR	0	0	0	0	0	0	*	*	0	*	*	*	*	0	*
Gradient	0	0	0	0	0	0	*	0	0	0	*	*	*	*	*
Vortex-Stretching	0	0	0	0	0	0	*	*	0	*	*	0	*	0	*

Table 22: Table 1 rearranged into the flow classes described in Section 4.4.1.

Dissipation Condition [Does $S_{ij}\tau_{ij}^{\mathrm{mod}}(v) = 0$?]

	$\mathcal{Q}_{7-9}$						$\mathcal{Q}_{0-6}$								
Solution	1	2	3	5	14	15	4	6	7	8	9	10	11	12	13
Smagorinsky	*	*	0	*	*	0	*	*	*	*	*	*	*	*	*
Vreman	0	0	0	*	0	0	*	*	*	*	*	*	*	*	*
QR	0	0	0	0	0	0	*	*	*	*	*	*	*	0	*
Gradient	0	0	0	0	0	0	*	*	*	*	*	*	*	*	*
Vortex-Stretching	0	0	0	0	0	0	*	*	0	*	*	0	*	0	*

Table 23: Table 2 rearranged into the flow classes described in Section 4.4.1.

Dissipation Condition 2 [Does $\overline{S}_{ij}\tau_{ij} = S_{ij}(\overline{v})\tau_{ij}^{\mathrm{mod}}(\overline{v})$?]

	$\mathcal{Q}_{7-9}$						$\mathcal{Q}_{0-6}$								
Solution	1	2	3	5	14	15	4	6	7	8	9	10	11	12	13
Exact	0	0	0	*	0	0	*	*	*	*	*	*	*	*	*
Smagorinsky	*	*	0	*	*	0	*	*	*	*	*	*	*	*	*
Vreman	0	0	0	*	0	0	*	*	*	*	*	*	*	*	*
QR	0	0	0	0	0	0	?	?	?	?	?	?	?	0	?
Gradient	0	0	0	0	0	0	*	*	*	*	*	*	*	*	*
Vortex-Stretching	0	0	0	0	0	0	*	*	0	*	*	0	*	0	*

Table 24: Table 4 rearranged into the flow classes described in Section 4.4.1.

C.2 Vreman's Zero-True-Subfilter-Dissipation Flow Classes

Velocity Field & Kinetic Energy Conditions [Do $\frac{\partial}{\partial x_j}\tau_{ij}^{\text{mod}}(v)$ and $v_i\frac{\partial}{\partial x_j}\tau_{ij}^{\text{mod}}(v)$ equal zero?]

	V_0				V_*										
Solution	1	2	3	14	4	5	6	7	8	9	10	11	12	13	15
Smagorinsky	0	*	0	*	*	*	*	0	*	*	*	*	*	*	0
Vreman	0	0	0	0	*	*	*	0	*	*	*	*	*	*	0
QR	0	0	0	0	*	0	*	0	*	*	*	*	0	*	0
Gradient	0	0	0	0	*	0	0	0	0	*	*	*	*	*	0
Vortex-Stretching	0	0	0	0	*	0	*	0	*	*	0	*	0	*	0

Table 25: Table 1 rearranged into the flow classes described in Section 4.4.2.

Dissipation Condition [Does $S_{ij}\tau_{ij}^{\text{mod}}(v) = 0$?]

	V_0				V_*										
Solution	1	2	3	14	4	5	6	7	8	9	10	11	12	13	15
Smagorinsky	*	*	0	*	*	*	*	*	*	*	*	*	*	*	0
Vreman	0	0	0	0	*	*	*	*	*	*	*	*	*	*	0
QR	0	0	0	0	*	0	*	*	*	*	*	*	0	*	0
Gradient	0	0	0	0	*	0	*	*	*	*	*	*	*	*	0
Vortex-Stretching	0	0	0	0	*	0	*	0	*	*	0	*	0	*	0

Table 26: Table 2 rearranged into the flow classes described in Section 4.4.2.

Dissipation Condition 2 [Does $\overline{S}_{ij}\tau_{ij} = S_{ij}(\overline{v})\tau_{ij}^{\text{mod}}(\overline{v})$?]

	V_0				V_*										
Solution	1	2	3	14	4	5	6	7	8	9	10	11	12	13	15
Exact	0	0	0	0	*	*	*	*	*	*	*	*	*	*	0
Smagorinsky	*	*	0	*	*	*	*	*	*	*	*	*	*	*	0
Vreman	0	0	0	0	*	*	*	*	*	*	*	*	*	*	0
QR	0	0	0	0	?	0	?	?	?	?	?	?	0	?	0
Gradient	0	0	0	0	*	0	*	*	*	*	*	*	*	*	0
Vortex-Stretching	0	0	0	0	*	0	*	0	*	*	0	*	0	*	0

Table 27: Table 4 rearranged into the flow classes described in Section 4.4.2.

C.3 Classes using the Third Principal Invariant

Velocity Field & Kinetic Energy Conditions [Do $\frac{\partial}{\partial x_j}\tau_{ij}^{\mathrm{mod}}(v)$ and $v_i\frac{\partial}{\partial x_j}\tau_{ij}^{\mathrm{mod}}(v)$ equal zero?]

	R_0									R_*					
Solution	1	2	3	5	8	11	12	14	15	4	6	7	9	10	13
Smagorinsky	0	*	0	*	*	*	*	*	0	*	*	0	*	*	*
Vreman	0	0	0	*	*	*	*	0	0	*	*	0	*	*	*
QR	0	0	0	0	*	*	0	0	0	*	*	0	*	*	*
Gradient	0	0	0	0	0	*	*	0	0	*	0	0	*	*	*
Vortex-Stretching	0	0	0	0	*	*	0	0	0	*	*	0	*	0	*

Table 28: Table 1 rearranged into the flow classes described in Section 4.4.3.

Dissipation Condition [Does $S_{ij}\tau_{ij}^{\mathrm{mod}}(v) = 0$?]

	R_0									R_*					
Solution	1	2	3	5	8	11	12	14	15	4	6	7	9	10	13
Smagorinsky	*	*	0	*	*	*	*	*	0	*	*	*	*	*	*
Vreman	0	0	0	*	*	*	*	0	0	*	*	*	*	*	*
QR	0	0	0	0	*	*	0	0	0	*	*	*	*	*	*
Gradient	0	0	0	0	*	*	*	0	0	*	*	*	*	*	*
Vortex-Stretching	0	0	0	0	*	*	0	0	0	*	*	0	*	0	*

Table 29: Table 2 rearranged into the flow classes described in Section 4.4.3.

Dissipation Condition 2 [Does $\overline{S}_{ij}\tau_{ij} = S_{ij}(\overline{v})\tau_{ij}^{\mathrm{mod}}(\overline{v})$?]

	R_0									R_*					
Solution	1	2	3	5	8	11	12	14	15	4	6	7	9	10	13
Exact	0	0	0	*	*	*	*	0	0	*	*	*	*	*	*
Smagorinsky	*	*	0	*	*	*	*	*	0	*	*	*	*	*	*
Vreman	0	0	0	*	*	*	*	0	0	*	*	*	*	*	*
QR	0	0	0	0	?	?	0	0	0	?	?	?	?	?	?
Gradient	0	0	0	0	*	*	*	0	0	*	*	*	*	*	*
Vortex-Stretching	0	0	0	0	*	*	0	0	0	*	*	0	*	0	*

Table 30: Table 4 rearranged into the flow classes described in Section 4.4.3.

C.4 Two-Component Flow Classes

Velocity Field & Kinetic Energy Conditions [Do $\frac{\partial}{\partial x_j}\tau_{ij}^{\mathrm{mod}}(v)$ and $v_i\frac{\partial}{\partial x_j}\tau_{ij}^{\mathrm{mod}}(v)$ equal zero?]

	C_2							C_3							
Solution	1	2	3	5	12	14	15	4	6	7	8	9	10	11	13
Smagorinsky	0	*	0	*	*	*	0	*	*	0	*	*	*	*	*
Vreman	0	0	0	*	*	0	0	*	*	0	*	*	*	*	*
QR	0	0	0	0	0	0	0	*	*	0	*	*	*	*	*
Gradient	0	0	0	0	*	0	0	*	0	0	0	*	*	*	*
Vortex-Stretching	0	0	0	0	0	0	0	*	*	0	*	*	0	*	*

Table 31: Table 1 rearranged into the flow classes described in Section 4.4.4.

Dissipation Condition [Does $S_{ij}\tau_{ij}^{\mathrm{mod}}(v) = 0$?]

	C_2							C_3							
Solution	1	2	3	5	12	14	15	4	6	7	8	9	10	11	13
Smagorinsky	*	*	0	*	*	*	0	*	*	*	*	*	*	*	*
Vreman	0	0	0	*	*	0	0	*	*	*	*	*	*	*	*
QR	0	0	0	0	0	0	0	*	*	*	*	*	*	*	*
Gradient	0	0	0	0	*	0	0	*	*	*	*	*	*	*	*
Vortex-Stretching	0	0	0	0	0	0	0	*	*	0	*	*	0	*	*

Table 32: Table 2 rearranged into the flow classes described in Section 4.4.4.

Dissipation Condition 2 [Does $\overline{S}_{ij}\tau_{ij} = S_{ij}(\overline{v})\tau_{ij}^{\mathrm{mod}}(\overline{v})$?]

	C_2							C_3							
Solution	1	2	3	5	12	14	15	4	6	7	8	9	10	11	13
Exact	0	0	0	*	*	0	0	*	*	*	*	*	*	*	*
Smagorinsky	*	*	0	*	*	*	0	*	*	*	*	*	*	*	*
Vreman	0	0	0	*	*	0	0	*	*	*	*	*	*	*	*
QR	0	0	0	0	0	0	0	?	?	?	?	?	?	?	?
Gradient	0	0	0	0	*	0	0	*	*	*	*	*	*	*	*
Vortex-Stretching	0	0	0	0	0	0	0	*	*	0	*	*	0	*	*

Table 33: Table 4 rearranged into the flow classes described in Section 4.4.4.

References

[1] D. J. Acheson. *Elementary Fluid Dynamics*. Oxford University Press, 1990. ISBN 0-19-859679-0.

[2] D. Barbato, L.C. Berselli, and C.R. Grisanti. Analytical and numerical results for the rational large eddy simulation model. *Journal of Mathematical Fluid Mechanics*, 9:44–74, 2007.

[3] R. Berker. *Intégration des équations du mouvement d'un fluide visqueux incompressible, Encyclopedia of Physics*, volume VIII/2 Fluid Dynamics II. Springer-Verlag, 1963.

[4] R.A. Clark, J.H. Ferziger, and W.C. Reynolds. Evaluation of subgrid-scale models using an accurately simulated turbulent flow. *Journal of Fluid Mechanics*, 91:1–16, 1979. doi:10.1017/S002211207900001X.

[5] L. Davidson. Fluid mechanics, turbulent flow and turbulence modeling. 2016. http://www.tfd.chalmers.se/~lada/MoF/lecture_notes.html Accessed: 17th May 2016.

[6] P.G. Drazin and N. Riley. *The Navier-Stokes Equations: A Classification of Flows and Exact Solutions*. Cambridge University Press, 2006.

[7] S. Irmay. New exact solutions of the Navier Stokes equations near a plane. *International Journal of Engineering Science*, 31:397–401, 1993. doi:10.1016/0020-7225(93)90014-L.

[8] B. Lautrup. *Physics of Continuous Matter: Exotic and Everyday Phenomena in the Macroscopic World*. Institute of Physics Publishing, 2005.

[9] A. Leonard. Energy cascade in large-eddy simulations of turbulent fluid flows. *Turbulent Diffusion in Environmental Pollution: Proceedings of a Symposium held at Charlottesville, Virginia, Advances in Geophysics*, 18 A:237–248, 1973.

[10] M. Oberlack. Invariant modeling in large eddy simulation of turbulence. *Centre for turbulence research*, 1997. arXiv:1510.07881[physics.flu-dyn].

[11] M.H. Silvis and R.W.C.P. Verstappen. Physically-consistent subgrid-scale models for large-eddy simulation of incompressible turbulent flows. 2015. arXiv:1510.07881[physics.flu-dyn].

[12] J. Smagorinsky. General circulation experiments with the primitive equations. *Monthly Weather Review*, 91:99–164, 1963. doi:10.1175/1520-0493(1963)091<0099:GCEWTP>2.3.CO;2.

[13] R.W.C.P. Verstappen. When does eddy viscosity damp subfilter scales sufficiently? *Journal of Scientific Computing*, 49:94–110, 2011. doi:10.1007/s10915-011-9504-4.

[14] R.W.C.P. Verstappen, S.T. Bose, J. Lee, H. Choi, and P. Moin. A dynamic eddy-viscosity model based on the invariants of the rate-of-strain. *Proc. Summer Program. Center for Turbulence Research, Stanford University/NASA Ames*, pages 183–192, 2010.

[15] R.W.C.P. Verstappen, W. Rozema, and H.J. Bae. Numerical scale separation in large-eddy simulation. *Proc. Summer Program. Center for Turbulence Research, Stanford University/NASA Ames*, pages 417–426, 2014.

[16] A.W. Vreman. An eddy-viscosity subgrid-scale model for turbulent shear flow: Algebraic theory and applications. *Physics of Fluids*, 16:3670–3681, 2004. http://dx.doi.org/10.1063/1.1785131.

[17] C.Y. Wang. Exact solutions of the steady-state Navier-Stokes equations. *Annual Review of Fluid Mechanics*, 23(1):159–177, 1991. http://dx.doi.org/10.1146/annurev.fl.23.010191.001111.